Impact of Degradation of the Moisture Separator on the Overall Performance of the Moisture Separator Reheater at a Nuclear Power Plant

Prepared by:

Natalie Saaymans

VNKNAT001

Department of Electrical Engineering

University of Cape Town

Supervisor: A/Prof Wim Fuls

December 2019

Submitted to the Department of Electrical Engineering at the University of Cape Town in partial fulfilment of the academic requirements for a Masters of Engineering degree in Nuclear Power.

Abstract

The moisture separator forms part of the moisture separator reheater (MSR) component used in a steam cycle in a nuclear power plant, to reduce the risk of erosion of the low-pressure (LP) turbine and to improve cycle efficiency. The performance and optimisation of moisture separators is well studied in literature; however, there have been few investigations on the impact of moisture separator degradation on MSR performance. To investigate this impact a mathematical model, representing the steam flow through the MSR, is developed and used to simulate and analyse the impact of degradation conditions.

The mathematical model was developed for design conditions, calibrated and validated against manufacturer specifications. The model was then augmented to include two moisture separator degradation conditions. The first degradation condition is the partial blockage of separator vane channels due to fouling, and the second is separator material deterioration resulting in steam bypass of the moisture separator. The model uses known properties of the MSR inlet steam and predicts the properties of steam exiting the MSR, given the simulated degradation of the moisture separator.

The outcomes of the model simulations demonstrated that partial blockage of moisture separator vane channels increases steam velocity though the separator and consequently improves MSR performance, but with a noted pressure drop. The velocity increased until a theoretical upper limit, above which re-entrainment of droplets back into the steam flow reduces MSR performance.

It was concluded that there is margin in the separator surface area design, where a minimal reduction in separator surface area (represented in the model as blockage of the vane channels) would improve the performance of the MSR, while still allowing for a buffer against the re-entrainment velocity upper limit. Equally, an unexpected improvement in MSR performance may be an indication of blockage of separator vane channels that, if not monitored and managed, could surpass the critical velocity limit where re-entrainment adversely affects the MSR performance.

The simulation results demonstrated that steam bypass of the moisture separator is a credible degradation condition which affects MSR performance. It was found that steam bypass of the moisture separator leads to a decline in the quality of steam exiting the separator and a decline in MSR performance. The simulation of a fully bypassed moisture separator showed that the MSR performance declines by more than three times the design value when compared to the scenario where there is no bypass of the moisture separator.

Declaration

I, Natalie Saaymans, hereby declare that I know the meaning of plagiarism and declare that all the work in the document, save for which is properly acknowledged, is my own. I have not allowed, and will not allow, anyone to copy my work with the intention of passing it off as their own work or part thereof. This thesis/dissertation has been submitted to the Turnitin module (or equivalent similarity and originality checking software) and I confirm that my supervisor has seen my report and any concerns revealed by such have been resolved with my supervisor.

Signed by candidate

Natalie Saaymans

Acknowledgements

I wish to acknowledge Eskom and the management of Nuclear Safety Assurance for nominating and sponsoring me for the Nuclear Power Master's degree. I am grateful to the management for releasing me from my responsibilities during the 2-year classroom modules. I must also acknowledge my colleagues who took over my roles and responsibilities during the periods when I was attending class.

I wish to thank the Eskom System Engineers, and particular Nazier Allie for assisting me with the necessary data and research material that was used in this study.

I thank my supervisor Dr Wim Fuls for provided me with guidance during my research. I also wish to thank him for reviewing my dissertation and for assisting me with programming relating obstacles.

I have pursued this dissertation and degree as a part-time student which, as a full-time employee, resulting in much family time being sacrificed. I thank my husband, Martin Saaymans for his encouragement, numerous reviews and for patiently being my sounding board. To my daughters Alexia and Scarlett, I hope that watching me toil and persevere through to the completion of this degree serves as motivation to further pursue their goals and ambitions.

I thank my parents, Alric and Carol van Niekerk for their constant, unwavering support of me and my aspirations. Without their sacrifices I would not be in the position to receive and pursue the opportunities I have been presented with.

Lastly, I would like to dedicate this dissertation to my brother, David van Niekerk, who tragically passed away during the course of this study. David's unrelenting drive to achieve, and constant encouragement of others to better themselves, has and will continue to inspire me.

Contents

List of Figures

List of Tables

Nomenclature

General symbols

A	Area of reheater (m^2)
b	Vane spacing (m)
d	Diameter
d_d	Droplet diameter (m)
C_F	Correction factor
f_T	Friction factor
h	Specific enthalpy of reheater steam, kJ/kg
h_{i+1}	Specific enthalpy of section i+1, kJ/kg
K_b	Bend coefficient
K_v	Liquid load factor
$\dot{m}$	Mass flow rate, kg/s
n	Number of reheater sections
n_b	Number of bends
P	Pressure
T	Temperature (K or °C)
T_{lm}	Log mean temperature across heat exchanger, K
U	Overall heat transfer co-efficient of reheater (W/m^2K)
v	Velocity (m/s)
w	Specific Work (kJ/kg)
Q	Heat transfer rate (kW)
x	Steam quality
z	Width of vane plate

Greek symbols

Δ	Difference or deviation
μ	Dynamic viscosity (Pa.s)
θ	Angle (°)
ρ	Density (kg/m^3)
η	Efficiency

Subscripts

c	Cold
c,in	Cold in
c,out	Cold out
cond	Conduction
conv	Convection
d	Droplet
ex	Exit
g	Vapour or gas
h	Hot
h,in	Hot in
h,out	Hot out
hs	Heating steam
in	Inlet
L	Liquid
RH	Reheater
sat	Saturation conditions

Acronyms and Abbreviations

CRT	Condensate recovery tank
EPRI	Electric Power Research Institute
HP	High-pressure
LMTD	Log mean temperature difference
LP	Low-pressure
MSR	Moisture separator reheater
OEM	Original equipment manufacturer
TTD	Terminal temperature difference

1 Introduction

A moisture separator forms part of the moisture separator reheater (MSR) component which is used in a steam cycle in a nuclear power plant to improve power cycle efficiency. An MSR improves power cycle efficiency by allowing the steam expansion to be split between a high-pressure (HP) and low-pressure (LP) turbine, with a reheat in-between. Steam from the HP turbine enters the MSR where excess moisture content is removed, and the steam is superheated before entering the LP turbine.

An MSR is comprised of a moisture separator and a heat exchanger or reheater. Packs of corrugated vane plates make up the moisture separator and the reheater is a condensing shell and tube design.

Moisture separator vane channels consist of several narrow spaced bended plates or vanes, angled to allow for drainage. Wet steam is forced through the constricted pathways where it repeatedly changes direction. Droplets in the steam, which are not able to follow the steam flow due to their inertia, impact on the vane walls, collect, and drain into drainage channels.

The performance and optimisation of moisture separators under various flow conditions and configurations is well studied in literature, both experimentally and numerically; however, there have been limited investigations on the impact of moisture separator degradation on overall MSR performance.

This research endeavours to create a mathematical model of the MSR for design conditions, augment the model to include two moisture separator degradation conditions, and then evaluate the impact of moisture separator degradation on overall MSR performance. The model will also determine the impact on the MSR performance should the moisture separator be completely bypassed.

The model is based on established mathematical principles of fluid and thermodynamics as well as published experimental studies of parameters affecting moisture separator performance. The software chosen to develop the model is Mathcad® and component specifications were obtained from a component manufacturer.

The two selected moisture separator degradation conditions are; blockage of the moisture separator channels due to fouling, and steam bypass of the moisture separator due to material deterioration of the separator plates. The research will consider the possibility for design improvements of the moisture separator as well as fault-finding considerations given a change in MSR output.

1.1 Objectives

The primary objective of the study is to develop a mathematical model of steam flow under design conditions through a moisture separator reheater. The model will then be augmented to include two moisture separator degradation conditions and enable an analysis of the impact the moisture separator degradation has on the performance of the MSR.

1.2 Scope and constraints of this study

The scope of the study made certain simplification assumptions in the construction of the model. These include:

- The model of the steam bypass assumes that the total surface area of the separator vanes remains approximately the same even though the material deterioration causing the bypass flow path would theoretically create a 'hole' in the surface area. This is a simplification, but the alternative would be to quantify the mass flow balance based on a specific size of the bypass hole, which in turn would require assumptions on the pressure drop characteristics of the hole. This is beyond the scope of the project.
- To obtain a value for maximum critical velocity, the liquid load factor, k_v, is required for the Souders-Brown equation. This value was not obtained from the original component manufacturer but is a supplier-recommended generic value for moisture separator units of similar design.
- The equation for pressure differential across the moisture separator vanes contains factors such as the friction factor f_T, and the bend coefficient for a 60° bend angle. The values for these factors were estimates obtained from engineering data on flow of fluids through pipes.
- It is assumed that the reheater UA is constant for every reheater section and does not change with flow or operating conditions. This assumption is a simplification used as, unless the actual heat transfer coefficient per reheater sections is calculated, this approach is the only feasible method for the scope of this study.
- Sub-cooling of the reheater heating steam condensate is disregarded in the model.

2 Theory

2.1 Heat exchangers

A heat exchanger is a component used for heat transfer between two fluids without mixing those two fluids. Heat is transferred from a hot fluid to a cold fluid via both conduction and convection processes through the wall separating them.

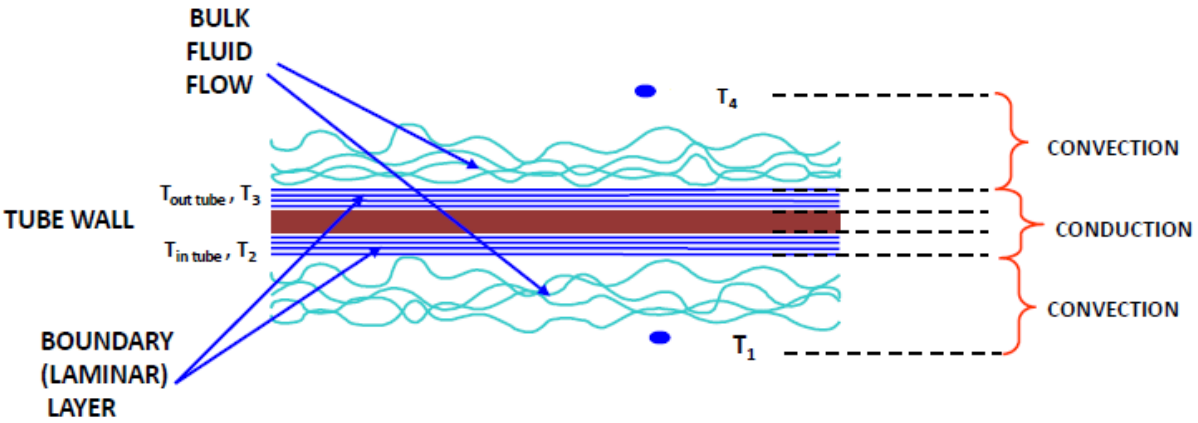

Figure 1: Heat transfer across heat exchanger tube [1]

In counter-flow heat exchangers, the hot and cold fluids flow in opposing directions and in parallel flow are in the same direction. Of the various flow arrangements, counter-flow has the highest thermal effectiveness. The conservation of mass principle dictates that for heat exchangers, the sum of the inbound mass flow rates equals the sum of the outbound mass flow rates. *[2]*

Condensing shell-and-tube heat exchanger

The shell-and-tube is the simplest and most common form of heat exchanger, consisting of inner pipes and an annular space between the shell and the inner pipes. One fluid flows in the inner pipes and the other in the annular space. Heat is transferred through the tube wall from the hot fluid to the cold fluid. In certain designs, the inner tube makes several turns inside the shell to increase the heat transfer area. Shell-and-tube heat exchangers are used in a wide range of industrial applications. *[3]*

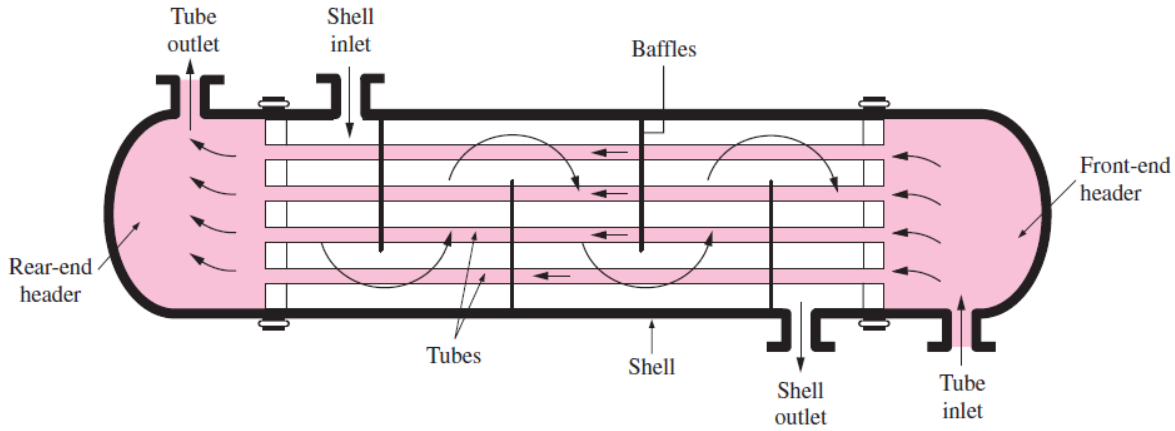

Figure 2: Shell and tube heat exchanger one-shell pass and one-tube pass [2]

Logarithmic mean temperature difference

Temperature difference is the effective driving force along the heat exchanger. The temperature difference between hot and cold fluids varies with position in the heat exchanger making it practical to calculate a mean temperature difference. Log mean temperature difference (LMTD) is the logarithmic temperature difference between hot and cold fluid streams and is defined in Equation 2-1.

$$\Delta T_{lm} = \frac{\Delta T_1 - \Delta T_2}{ln\frac{\Delta T_1}{\Delta T_2}} \qquad 2\text{-}1$$

ΔT_1 and ΔT_2 represents the temperature difference between the two fluids at the two ends (inlet and outlet) of the heat exchanger. It makes no difference which end of the heat exchanger is designated as the inlet or the outlet. [2]

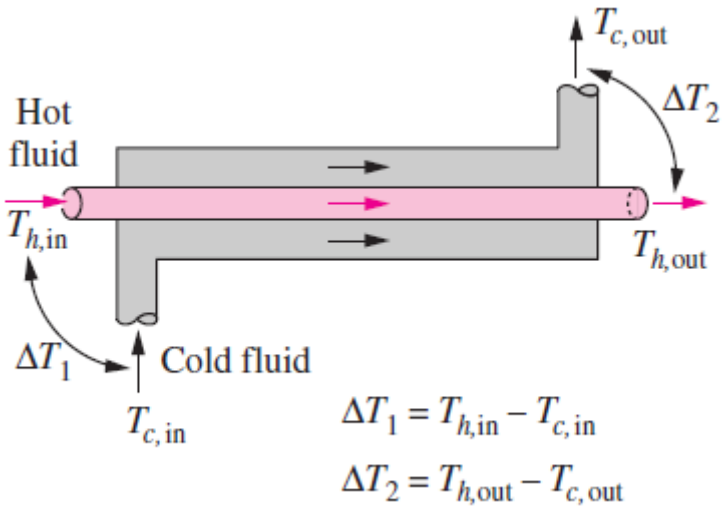

Figure 3: Expressions for ΔT_1 and ΔT_2 in parallel-flow heat exchanger [2]

LMTD is used in Equation 2-2 to calculate the heat exchanger overall heat transfer. Equation 2-2 is commonly referred to as the log mean temperature difference formula and is a basic equation for heat exchanger design.

$$Q = UA\Delta T_{lm} \qquad 2\text{-}2$$

Where

Q = heat transfer (kW)

U = heat transfer coefficient (kW/m^{2}K)

A = heat transfer surface area (m^2)

ΔT_{lm} = log mean temperature difference (K)

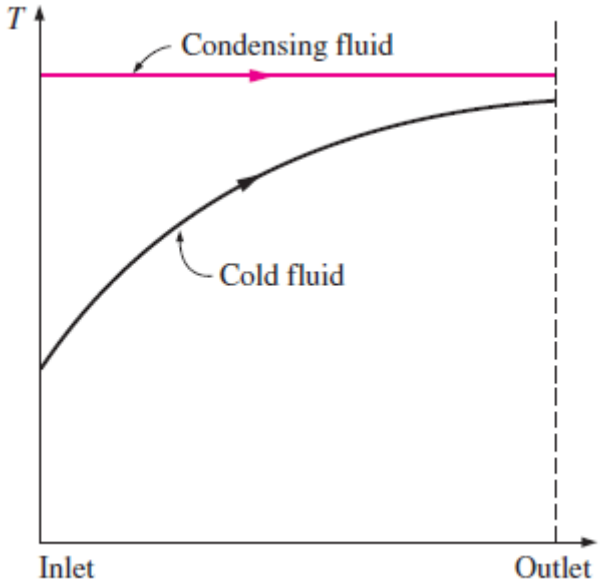

Figure 4: Condensing heat exchanger temperature profile [2]

Figure 4 shows the expected heat exchanger temperature profile for a condensing heat exchanger. The mean temperature difference between the two fluids is logarithmic in nature and the average temperature difference between the hot and cold fluids can therefore be determined by using the LMTD method as reflected in Equation 2-1.The LMTD method is limited to parallel-flow, counter-flow and single stream heat exchangers.

For complex flow conditions a correction factor, F, is introduced into the log mean temperature difference formula, and depends on the geometry of the heat exchanger whether there is mixture of the flow per stream, as well as the heat capacity ratio of the two streams.

For the configuration modelled in this study, the correction factor F is not used as the heat exchanger modelled is a single stream condensing heat exchanger. [2]

The LMTD method does not account for phase changes such as evaporation and superheating in the heat exchanger and therefore cannot be used to accurately calculate the heat transfer for a heat exchanger where these phase changes take place.

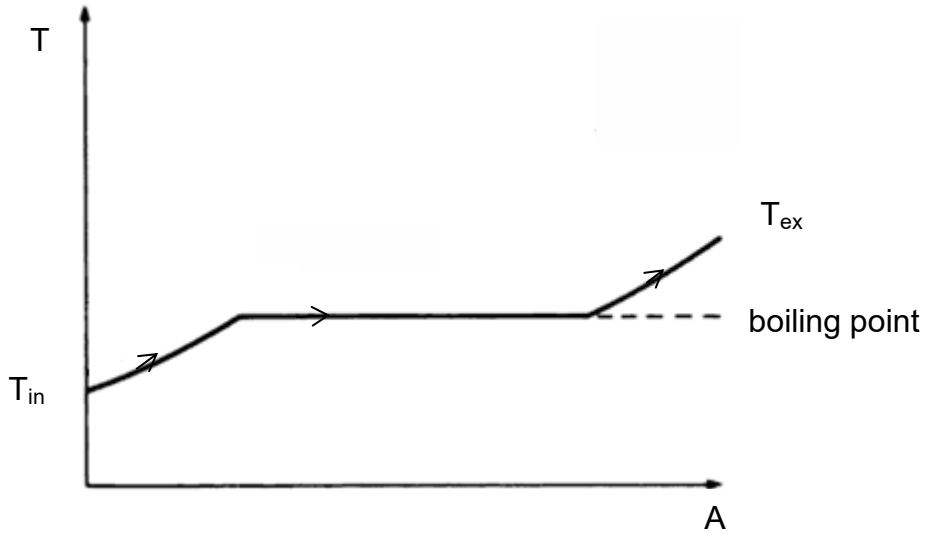

Figure 5: Heat exchanger temperature profile with a change in phase [4]

Figure 5 shows the temperature profile in a heat exchanger where the temperature of the steam increases during preheating to the fluid boiling point, then remains constant as the excess moisture in the steam is evaporated, followed by an increase in temperature where the dry steam is superheated.

During a phase change, heat is transferred without affecting the temperature of the fluid and consequently the specific heat appears to be infinite. Due to the rapid change in the specific heat at the point of phase change, the LMTD calculation for heat transfer cannot be accurately used. The LMTD method assumes that the temperature and fluid properties are uniform over every flow cross-section. [4]

The difficulty in modelling a heat exchanger where the fluid is heated, evaporated, and superheated, is the continuous variation of overall heat transfer coefficient with position in the heat exchanger. If the three parts of the heat exchanger had constant values of overall heat transfer coefficient, then the heat exchanger could be treated as three different heat exchangers in series. [5] Alternatively, one would need to discretise the heat exchanger, and analyse each section separately.

The overall heat transfer coefficient

Heat transfer in a heat exchanger involves convection in each fluid and conduction through the wall separating the two fluids. When analysing heat exchangers it is convenient to work with the overall heat transfer coefficient which accounts for the effects of conduction and convection and is equal to the inverse of the total thermal resistance.

$$UA = \frac{1}{R_{Total}} \qquad 2\text{-}3$$

Figure 6 and Equation 2-4 [2] represents the total thermal resistance through a wall. Given Equation 2-3 [2] and assuming negligible pipe wall thickness and equal inner and outer area, it can be seen that the overall heat transfer coefficient is made up of the inverse sum of internal and external convection. Internal convection is strongly dependant on fluid properties such as density, viscosity and velocity and the dominant driver for condensing heat transfer on the outside of the tubes is temperature gradient (Equations 2-5 and 2-6).

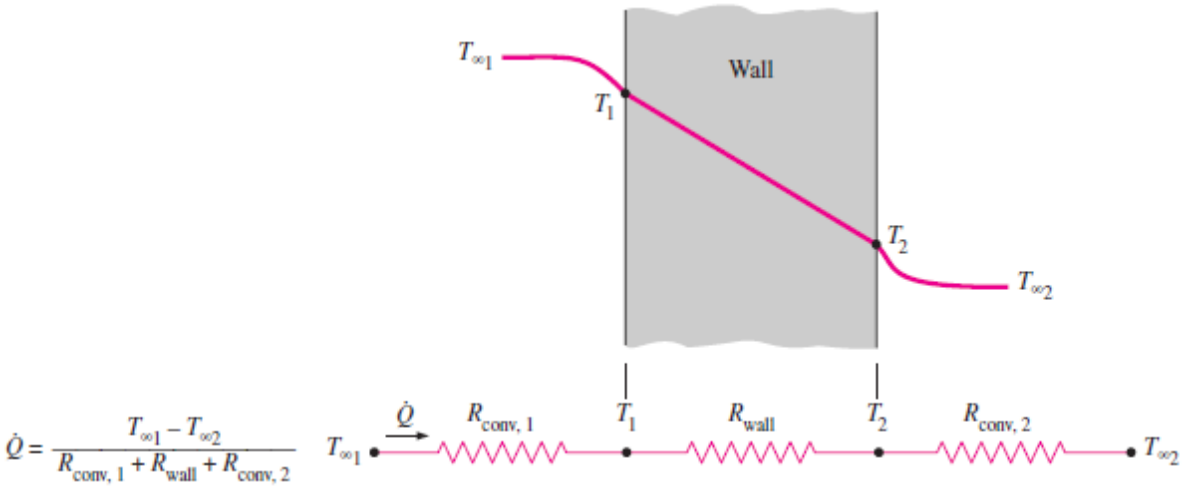

Figure 6: The thermal resistance network for heat transfer through a plane wall subjected to convection on both sides. [2]

$$R_{Total} = R_{conv1} + R_{wall} + R_{conv2} = \frac{1}{h_1 A} + \frac{L}{kA} + \frac{1}{h_2 A} \qquad 2\text{-}4$$

The internal convective coefficient can be calculated using the Dittus-Boelter correlation for forced convection in pipes and ducts. The Reynolds number in this equation is calculated using the flow rate of the liquid phase alone. [6]

$$Nu = 0.023 Re^{0.8} Pr^{0.4} \qquad 2\text{-}5$$

Where:

Nu = Nusselt number

Re = Reynolds number for Re > 10 000, Re = $\frac{\rho V L_c}{\mu}$

Pr = Prandtl number 0.7 ≤ Pr ≥160, Pr = $\frac{\mu Cp}{k}$

n = 0.4 for heating and 0.3 for cooling of the fluid flowing through the tube

The fluid properties are evaluated at the bulk mean fluid temperature; $T_b = \frac{T_i + T_e}{2}$

For the condensing heat transfer on the outside of the tubes the dominant driving force is the temperature difference between the wall surface and the bulk temperature of the saturated vapour as seen in equation 2-6 [6]

$$h = 0.728 \left[\frac{k_L^3 \rho_L (\rho_L - \rho_v) g \gamma}{\mu_L (T_v - T_w) D_o} \right]^{1/4} \qquad 2\text{-}6$$

Where:

γ = the latent heat of vaporisation

G = gravitational acceleration

D_o = pipe outer diameter

ρ = density

μ = viscosity

T_v = vapour temperature

T_w = wall temperature

k_L = thermal conductivity of liquid

2.2 Power plant steam systems

Steam has many positive characteristics such as a high enthalpy of vaporisation, availability, and low cost, making it the most common process fluid used in vapour power cycles. In a nuclear pressurised water reactor steam cycle, there is heat addition in the steam generator, expansion in the turbine, heat rejection in a condenser, and compression in a feed pump. Water enters the feed pump as saturated liquid and is compressed to the operating pressure of the steam generator. Water enters the steam generator as a compressed liquid and exits as saturated steam vapour. The vapour enters the turbine, where it expands and produces work by rotating the shaft connected to an electric generator. The pressure and temperature of the steam drop during the process, after which the steam enters the condenser. At this point in the process the steam is usually a saturated liquid-vapour mixture. Steam is condensed at constant pressure in the condenser by rejecting heat to a cooling medium. Steam leaves the condenser as a saturated liquid and enters the feed pump, completing the cycle. [7]

A method to increase the efficiency of the steam cycle is to reheat and superheat the steam. Superheating steam to higher temperatures increases thermal efficiency and decreases the moisture content of the steam at the turbine exit.

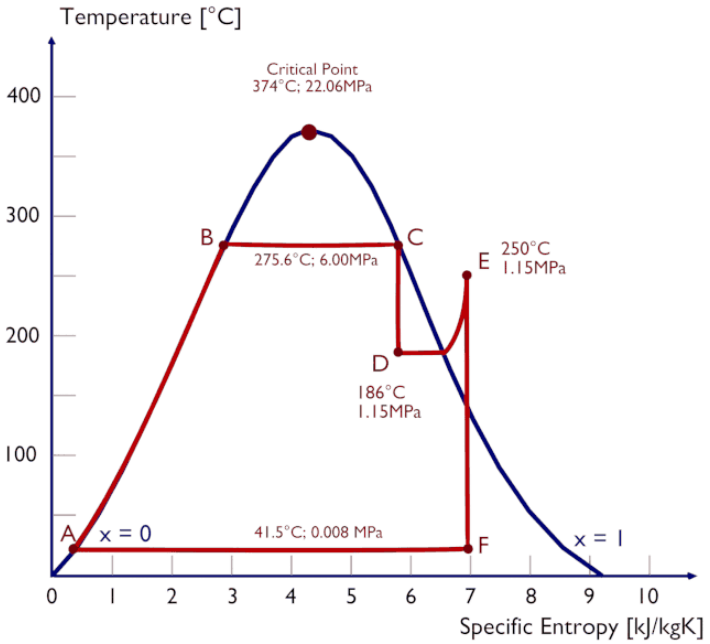

Figure 7: The Rankine cycle in a nuclear power plant [8]

The purpose of the reheat cycle, depicted in Figure 7, is to reduce the moisture content of the steam at the final stages of the expansion process. In the absence of a reheat cycle, an option is to superheat the steam to very high temperatures to eliminate the problem of excessive moisture; however, there are metallurgical

constraints to this solution. Another option would be to operate at lower pressures but with a corresponding drop in cycle efficiency.

Reheating is commonly used in modern steam power plants as a practical solution to the excessive moisture problem in turbines. In a reheat cycle the steam is expanded in the turbine in two stages with a reheat in-between. [7]

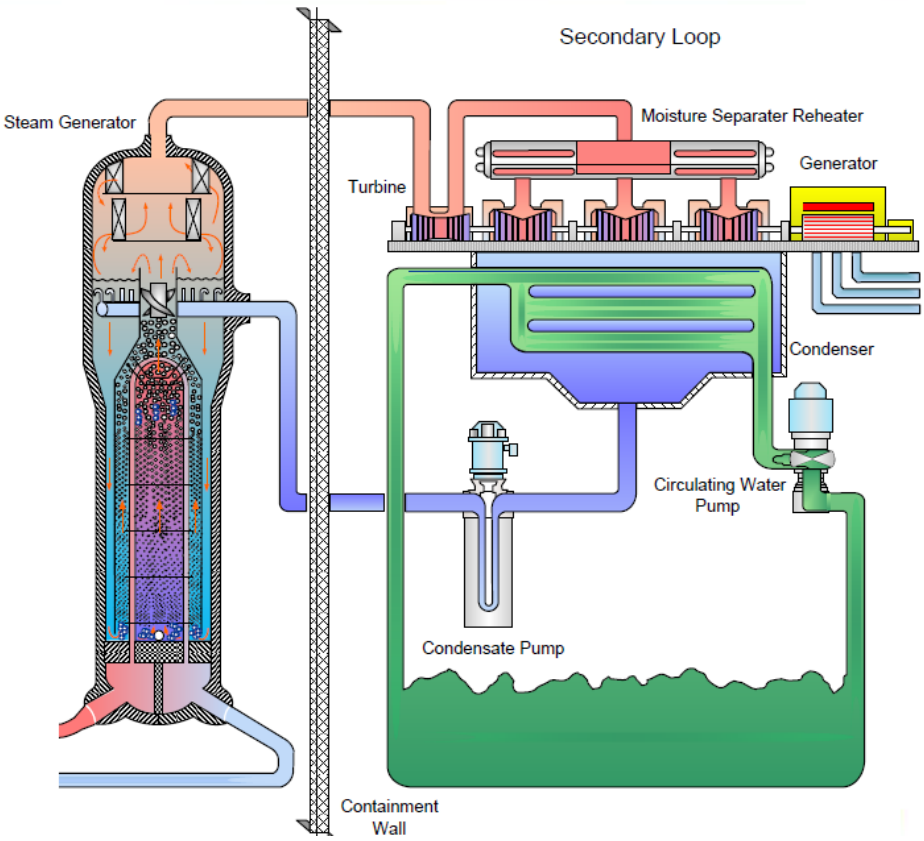

Figure 8: Secondary steam loop in a nuclear power plant [1]

In the secondary loop in a light water nuclear power reactor, the steam generator produces saturated steam, not superheated steam, which is fed to the high-pressure turbine. Following the steam expansion in the HP turbine, the MSR removes the excess moisture and superheats the steam before it is fed to the low-pressure turbine.

3 Literature Review

Moisture separator reheaters (MSRs) are used in the nuclear power generation industry in the secondary steam cycle to remove water droplets in wet steam exhausted from the high-pressure (HP) turbine and provide dry, heated (superheat) steam to the low-pressure turbine (LP).

A reduction in moisture content increases the turbine mechanical efficiency and reduces the potential for erosion or corrosion damage in the low-pressure turbine.

It is accepted that, in order to minimise damage to the turbine, a separation efficiency of 99,9% is required. [9]

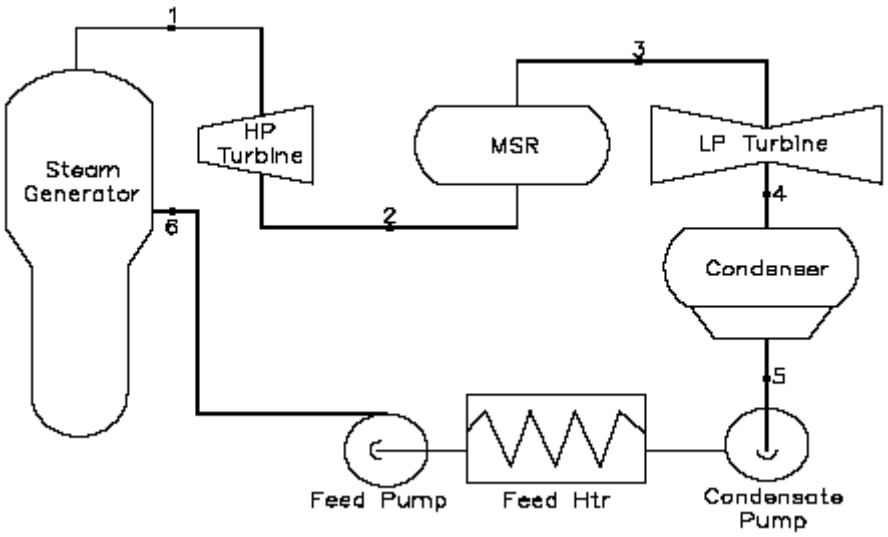

Figure 9: Simplified version of the major components of a typical steam plant cycle [10]

1-2: Saturated steam from the steam generator is expanded in the high-pressure (HP) turbine to provide shaft work output at constant entropy.

2-3: The moist steam from the exit of the HP turbine is dried and superheated in the moisture separator reheater (MSR).

3-4: Superheated steam from the MSR is expanded in the low-pressure (LP) turbine to provide shaft work output at constant entropy.

4-5: Steam exhaust from the turbine is condensed in the condenser in which heat is transferred to the cooling water under a constant vacuum condition.

5-6: The feed water is compressed as a liquid by the condensate and feed pump and the feed water is preheated by the feed-water heaters.

6-1: Heat is added to the working fluid in the steam generator under a constant pressure condition.

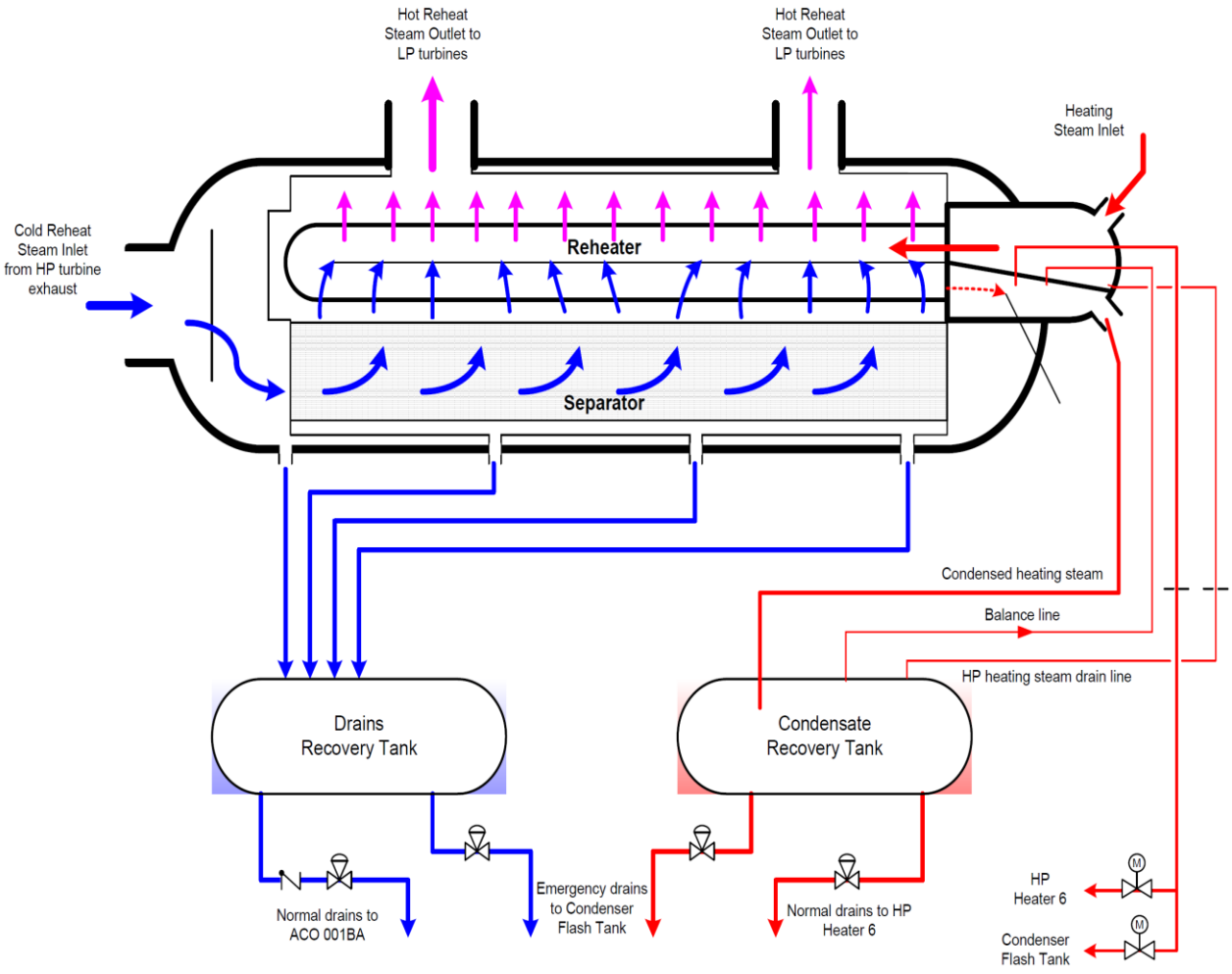

Figure 10: Moisture separator reheater steam flow with heating steam path and condensate drain [11]

3.1 Moisture separator reheater (MSR)

The moisture separator reheater studied, as shown in Figures 10, 11, 12 and 13 is 15,56 m in length and 3,1 m in diameter and is orientated in the horizontal position. The vessel is designed to contain moisture separator equipment and tube bundles used to reheat the cycle steam. The vessel is larger than the tube bundles in order to produce cycle steam velocities needed for efficient moisture separation by surface contact.

The MSR vessel has large piping connections, including one for inlet cycle steam at one end and several outlet steam connections on the top of the cylindrical part of the vessel. The multiple outlet nozzles aid in distributing cycle steam flow uniformly across the moisture separators and reheat tube bundles and provide multiple feeds to the LP turbine. [12]

The cycle steam inlet of nearly all MSRs is at one end or the bottom of the vessel. The steam flows through the moisture separators that are distributed along the length of the vessel. [12]

Figure 11: Moisture separator reheater at a nuclear power plant [11]

The EPRI moisture separator source book states that in MSRs high moisture removal efficiency is needed to fully utilise the reheater surface to reheat steam, rather than to evaporate residual moisture in the cycle steam. Steam expands across the HP turbine and consequently increases the moisture content to approximately 10-15% at the HP turbine exhaust. [12]

A system with just a moisture separator will experience a gain in cycle efficiency of 4 to 5%, whereas a system with a moisture separator and a reheater will achieve a 6 to 7% gain in cycle efficiency. [12]

The separator performance will directly affect the reheater performance as 1% water content at the separator outlet will require 10% increase in heating steam for evaporation of the water content. [13]

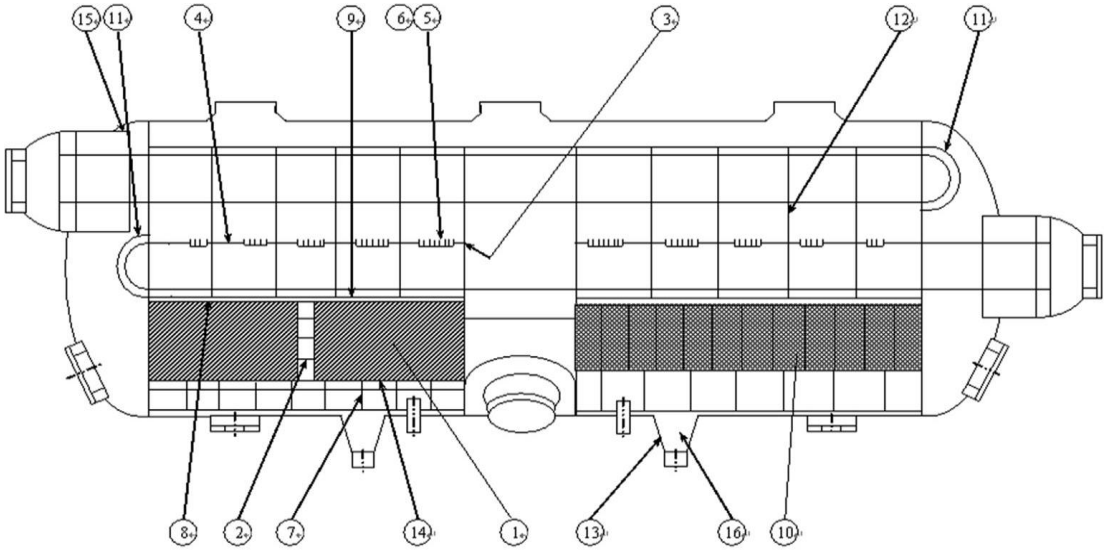

Figure 12: Structure of a moisture separator reheater, horizontal cross-section view [14]

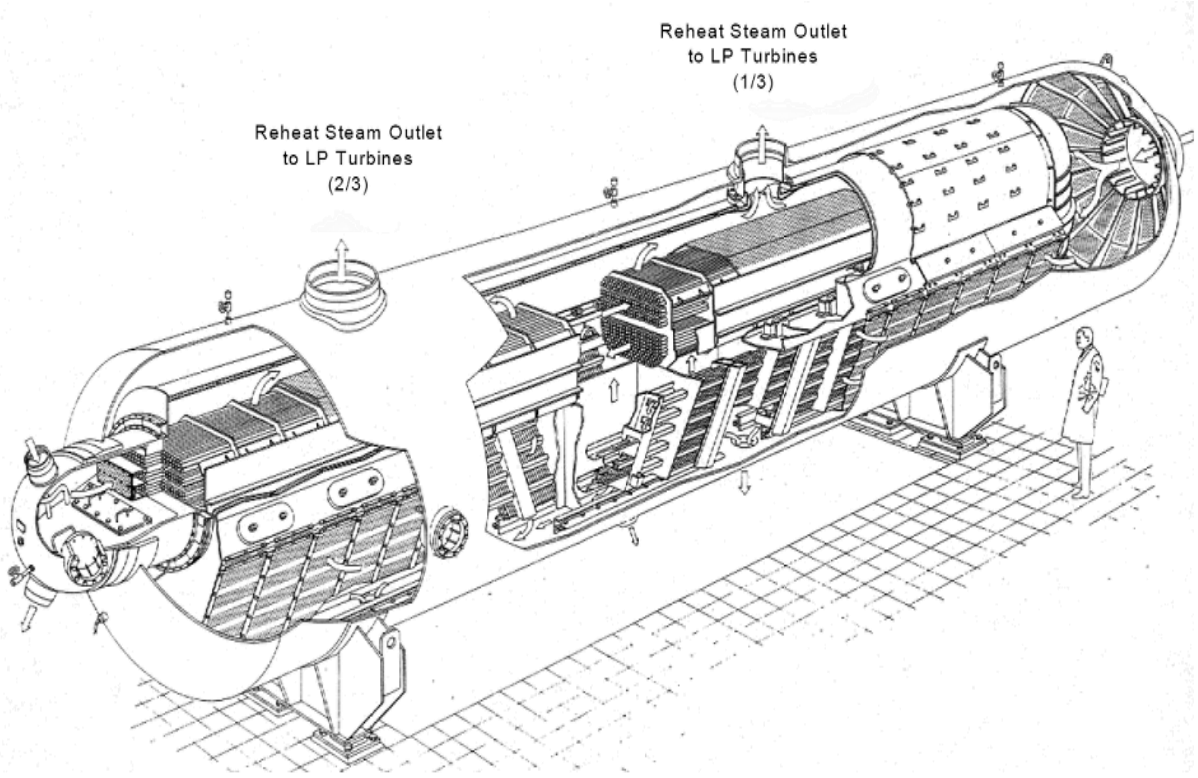

Figure 13: Layout and scale of MSR [11]

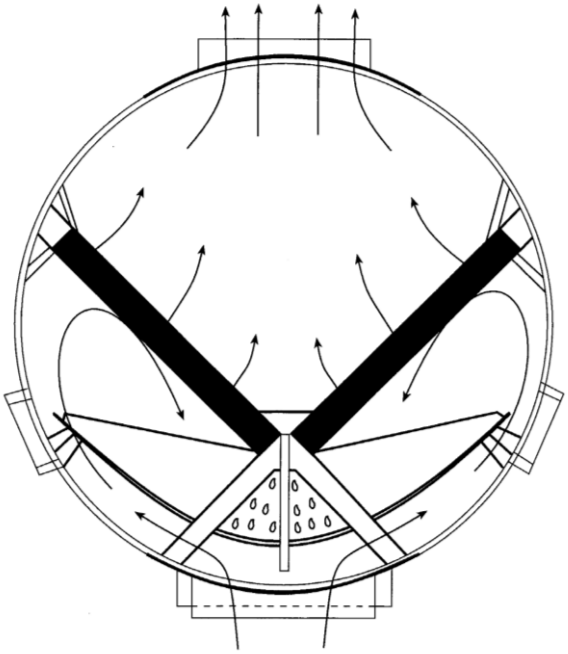

Figure 14: Cross-sectional view of a horizontal moisture separator reheater [12]

In Figure 14, the steam flows from the bottom of the vessel from where it is pushed through the moisture separator vanes (coloured in solid black) and into the re-heating space, where the heat exchanger tube bundles are situated. Dry superheated steam then exits at the top of the vessel.

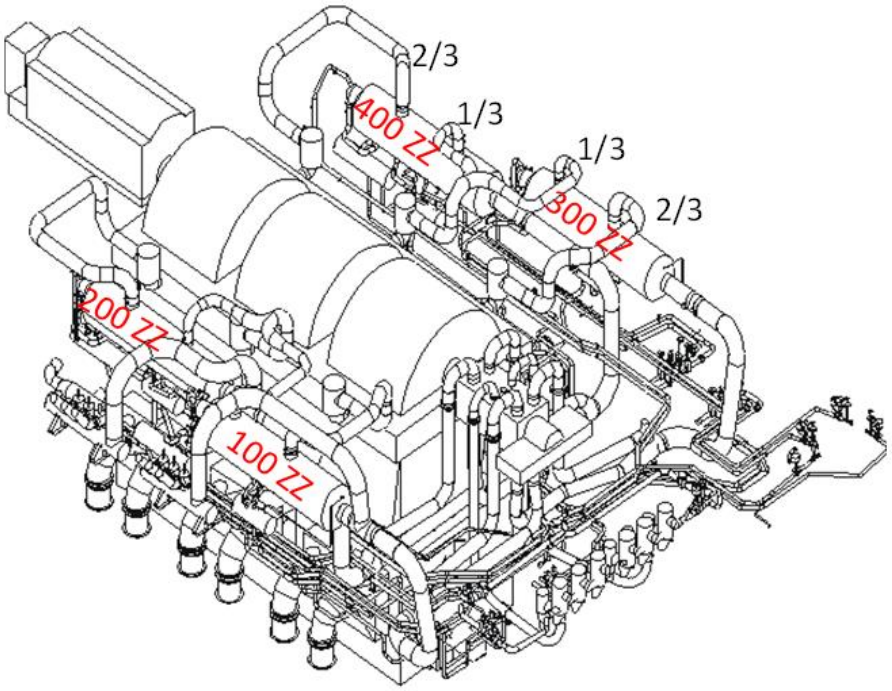

Figure 15: Illustration of MSR configuration around turbine centreline [11]

The power plant on which the model is based has four MSR units situated around the LP turbine centreline (Figure 15). A steam box ensures the distribution of heating steam to the tubes. The water resulting from this condensation is collected by gravity to the condensate recovery tank (CRT). Perforated plates are installed in front of the tube inlets in order to reduce the sub-cooling of the lower tube branches.

3.2 Moisture separator

Moisture separators with corrugated plates are widely used in nuclear power plants because of its efficiency and low resistance. The working principles of the separators are primarily based on the difference in inertia between steam and water droplets Separation happens by inertial impingement. Due to their relatively large inertia, the droplets do not adjust trajectory to the change in the curved streamlines in the wave channel and impinge and deposit on the wall. The separated droplets form a water film on the wall of the plates. The droplets then drain down along the wall of the corrugated plates to the drain channel at the end of the separation block. After passing through the moisture separator the cycle steam contains a quantity of residual water varying from 0,1 to 1% mass, dependent on the separating efficiency, turbine load, and operating conditions. [15]

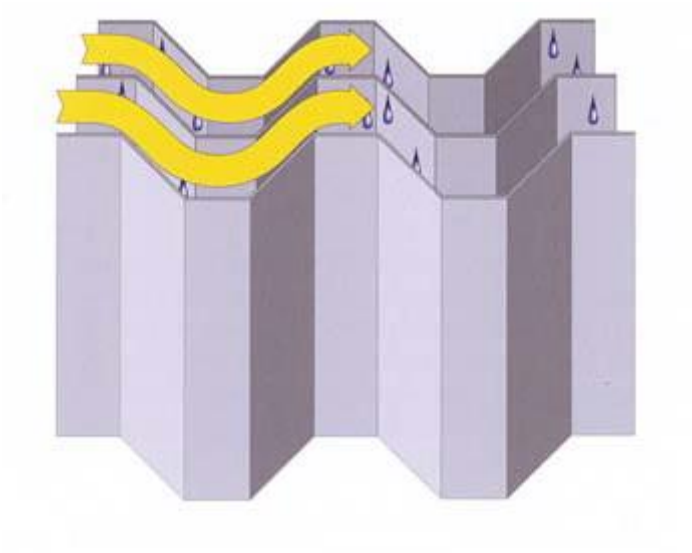

Figure 16: Wet steam flow through separator vanes [16]

As seen in Figures 16 and 17, the winding travel path that the corrugated vane plates provide, forces the steam to navigate through tight curves. As the steam changes direction, inertia and momentum keep the droplets moving in a straight path resulting in the impact of some droplets onto the vane surface. Having collided with the material surface, the droplets are held there by forces of adhesion between the water and the surface. Droplets then merge to eventually run down the vanes into a drainage channel. [9]

The mass fraction of water droplets at the inlet of the separator is in the range of 5 to 25% which is a volume fraction of less than 10%. The droplet is therefore treated as isolated and it can be assumed that the fluid influences the droplets via drag and turbulence, but the droplets have no influence on the gas flow. [17]

The flow in a wave-type channel is often laminar, even though the hydraulic Reynolds number might appear high. Curved passages tend to delay the onset of turbulence, which has been experimentally observed in work with corrugated plate moisture separators. [18]

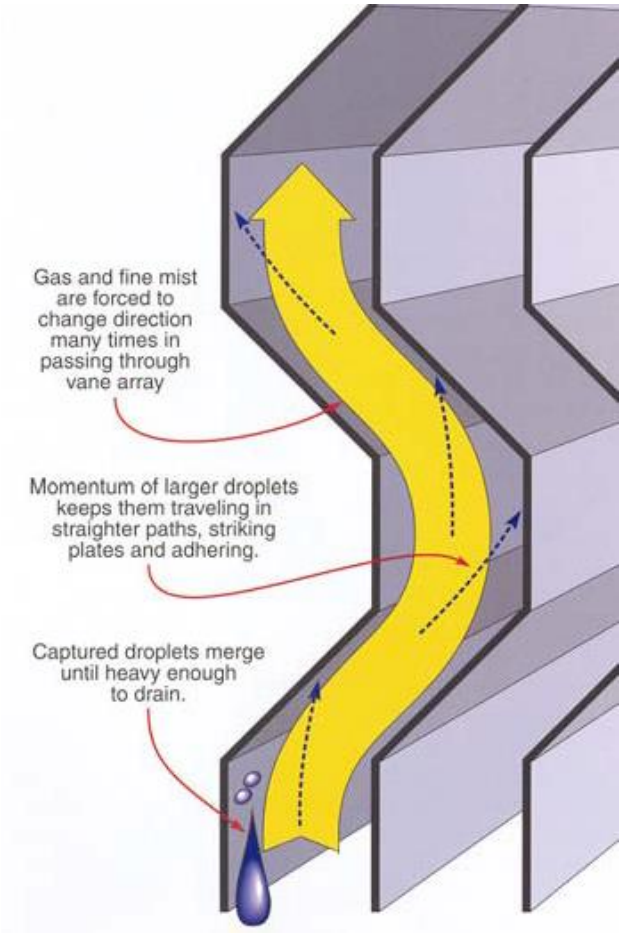

Figure 17: Depiction of droplet removal mechanism [16]

The most common form of moisture separator is the chevron vane type shown in Figure 17. The vanes provide a large amount of contact surface to collect moisture and are usually orientated vertically or are inclined to provide a drain path to the bottom of the MSR vessel, which minimises re-entrainment of water into the dry steam path. [12]

Wave-plate separators are typically less efficient in removing very small droplets (< 10 μm) compared to other types of separators such as cyclones; however, they usually have a low pressure drop and can collect up to 100% of droplets greater than 10 μm depending on the design parameters. Regarding the performance of separators, two parameters are important, namely the drop in pressure of the gas across the separator, and droplet removal efficiency. The pressure drop and droplet removal efficiency of separators are a function of its geometrical and steam property parameters which include plate spacing, bend angle, number of bends in each plate, and velocity of steam. [19]

Figure 18: Typical vane packs or blocks [20]

The moisture separator unit modelled is assembled in blocks similar to those in Figures 18 and 19. In Figure 20 blocks of the modelled moisture separator is viewed from the manway at the top of the MSR vessel. Each block consists of 120 to 128 corrugated sheets and is kept in place by two end plates using four bracing rods welded and made flush on the outer faces. The two end plates have holes to bolt them to the equipment. The slope of the plates is 60˚ to the horizontal to allow drainage of the water. A plate forming an angle piece is welded onto the separation block, ensuring sealing between the inlet steam and the dry steam. [11] The gap between plates is between 12 and 20 mm. [21]

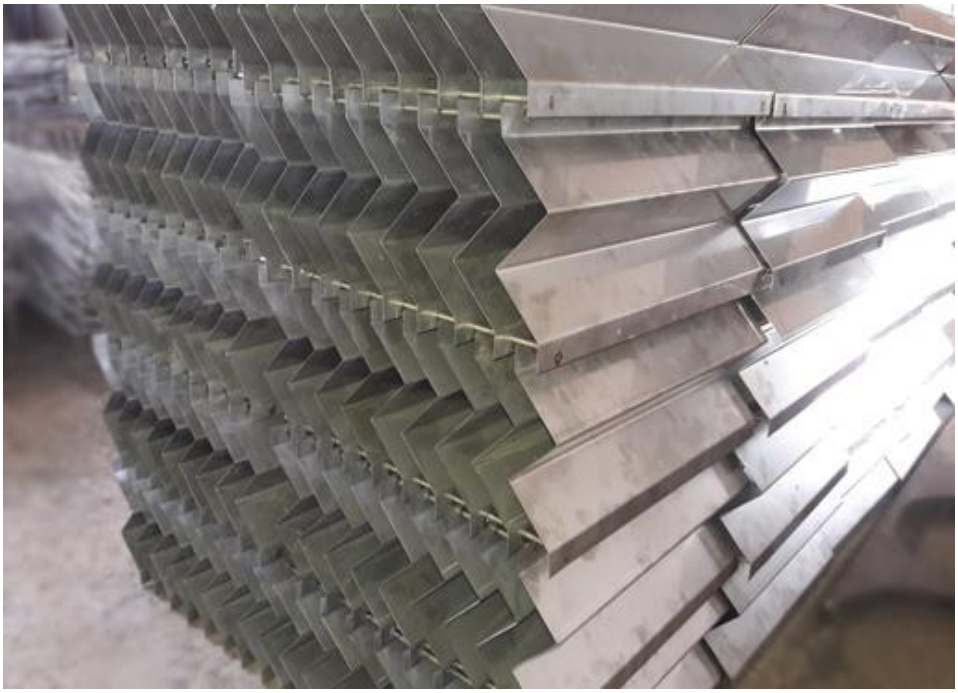

Figure 19: Moisture separator vanes made of stainless steel [22]

Figure 20: Moisture separator blocks in vessel, viewed from the manway at the top of the vessel looking down [undisclosed source]

Typical MSR shell-side degradation

Most MSRs are provided with manways which provide access to visually inspect the shell-side moisture separators and reheater tube bundles when the plant is shut down. Shell-side visual inspections can be used to determine whether one or more of the following types of damage has occurred:

- Erosion and moisture damage to demister pads and chevron separators;
- Erosion and moisture damage to inlet cycle steam passageways and manifolds;
- Deposits between tube fins due to moisture carry-over;
- Corrosion/erosion of carbon steel reheater finned tube surface;
- Cracked welds in partitions and other plate components;
- Erosion damage to carbon steel components downstream of stainless-steel weld deposits applied to prevent erosion;
- Openings between cold and hot cycle steam sections of the MSR;
- Gaps allowing bypass of cycle steam around moisture separator panels;
- General area erosion as evidenced by wall thinning and changes in the texture and colour of carbon steel surfaces in the cold cycle steam path. [12]

Blocking of the moisture separator vanes

As minerals or debris deposit on the vane material, the vane channel diameter available for steam flow decreases and becomes blocked. To mathematically simulate this condition and the effects on moisture separator efficiency, a surface area blockage ratio can be formulised and its impact on velocity, pressure, and enthalpy determined.

Bypass of the moisture separator

The bypass flow defect is based on the scenario of material deterioration resulting in a ‘hole’ in the separator vane pack which becomes the bypass flow path. Figure 21 demonstrates the condition schematically.

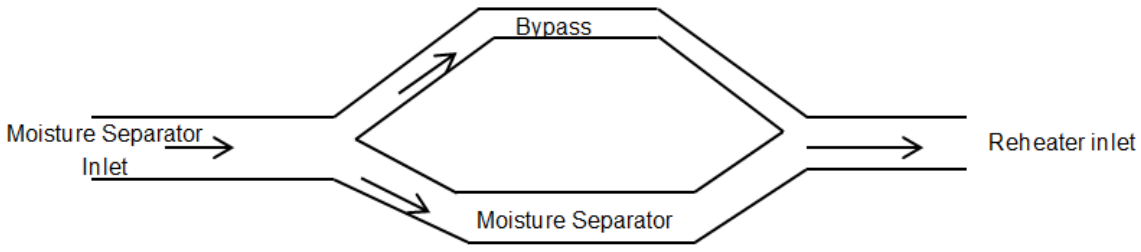

Figure 21: Moisture separator bypass flow schematic

To determine the remaining mass of steam flowing through the moisture separator, a mass flow bypass ratio can be formulated.

The bypass flow contains the same moisture content as the flow exiting the high-pressure turbine. The bypass mixes with flow exiting the moisture separator to give a certain steam quality which enters the reheater. The new quality can be calculated either by using a mass balance or by adding the separate enthalpies and quality for the bypass and moisture separator streams.

Moisture separator pressure differential

Pressure differential across the moisture separator vanes is impacted by flow dynamics through the vane as represented in Equation 3-1 [23].

$$\Delta \mathrm{P} = \sum_{i=1}^{n} f_D \left(\frac{A_d}{A_T}\right) \rho_g \left(\frac{v_g}{2}\right) \qquad 3\text{-}1$$

ΔP = pressure differential over moisture separator

f_D = drag coefficient for a plate inclined at angle Θ

ρ_g = density of gas

v_g = superficial gas velocity

n = number of rows of baffles

A_D = frontal area

A_T = total flow cross sectional area

Moisture separators can become fouled with minerals or debris. Data obtained through practical experimentation with vane moisture separators indicate a rapid increase in pressure differential as the vane channel is fouled or blocked up. As materials build up on the plates, the local velocities increase due to the restrictions of open area which substantially reduces the pressure. [24]

Moisture separator removal efficiency

Monat et al [24] investigated the quantification of moisture separator droplet removal efficiency using laser-based droplet sizing interferometer and established the separator geometrical and gas properties that affect removal efficiency; such as gas velocity, plate spacing, bend angle and the number of bends in each plate. Equation 3-2 is a representation of these factors.

$$\eta(d_d) = 1 - \exp\left[\frac{-(\rho_d d_d^2 v_g n_b \theta)}{515.7 \mu_g b \cos^2\theta}\right] \quad 3\text{-}2$$

Where:

- $\eta(d_{d)}$ = fractional removal efficiency of droplets of diameter, d_d
- d_d = droplet diameter
- ρ_d = droplet density
- μ_g = gas viscosity
- v_g = gas superficial velocity
- θ = bend angle
- n_b = number of bends
- b = vane spacing

These parameters affect the performance of moisture separators where, for example; increasing the number of bends will also improve the collection efficiency but increase the gas pressure loss, decreasing the plate spacing will increase the droplet collection efficiency with no effect on the pressure differential, and increasing the gas velocity improves collection efficiency but with a loss in gas pressure.

Re-entrainment

In moisture separators there is a velocity upper limit of the gas flowing across the surface of the entrained liquid, to prevent re-entrainment of the liquid into the gas phase. Re-entrainment of coalesced droplets occurs above a certain critical velocity, when drag forces, gravitational forces, and surface tension forces combine in such a way that droplets detach from the vanes and are carried downstream by high-velocity gas flow. Generally, droplets formed near the inlet of the separator are removed before they reach the outlet, but eventually the liquid holdup reaches the outlet region where detached droplets cannot be removed downward and appear as re-entrainment at the outlet of the separator. [24]

To prevent re-entrainment, the separator must be designed and sized such that the design velocity is below the critical velocity.

At high gas velocities, a separator can have a theoretical removal efficiency of 100% and simultaneously re-entrain extensively. Conversely, at low gas velocities the separator may not re-entrain but have poor removal efficiency. In the case of lower velocities, droplets have low momentum and as such can better navigate the winding vanes and avoid impingement on the vane surface. At relatively high velocities, the vapour has enough kinetic energy to re-entrain removed droplets. As the velocity

decreases, the droplet capture efficiency declines more steeply for smaller droplets than for larger ones. At some point, the efficiency for droplets at the lower end of the size range has fallen to an unacceptable level. This is the bottom of the operating velocity range. [24] Optimal separator efficiency is achieved at a gas velocity that is as high as possible but not so high that it yields re-entrainment.

To obtain a value for maximum critical velocity, the Souders-Brown equation is used [16]. The liquid load factor used is a recommended value for a vane moisture separator unit of similar design to the modelled separator.

$$v_g = K_v \sqrt{\frac{\rho_L - \rho_g}{\rho_g}} \qquad 3\text{-}3$$

Where:

v_g = maximum allowable vapour velocity

K_v = liquid load factor

ρ_L = density of liquid

ρ_g = density of gas

4 Model development

A mathematical model of steam flow through an MSR is created using Mathcad®. The model represents steam flow exiting the high-pressure turbine, through the moisture separator reheater and to the inlet of the low-pressure turbine.

The model is created for design conditions, calibrated and then validated against manufacturer specifications. It is then augmented to include two moisture separator degradation conditions. The model contains a sequence of integrated calculations describing the thermodynamic and flow dynamic processes of the steam within the MSR i.e. through the moisture separator and reheater.

4.1 Modelling MSR design conditions

The model is first developed to simulate design conditions within the MSR using the known MSR inlet and exit steam parameters. The moisture separator exit quality for design conditions is determined as a function of the separator inlet quality and mass flow rate as well as the reheater inlet mass flow rate.

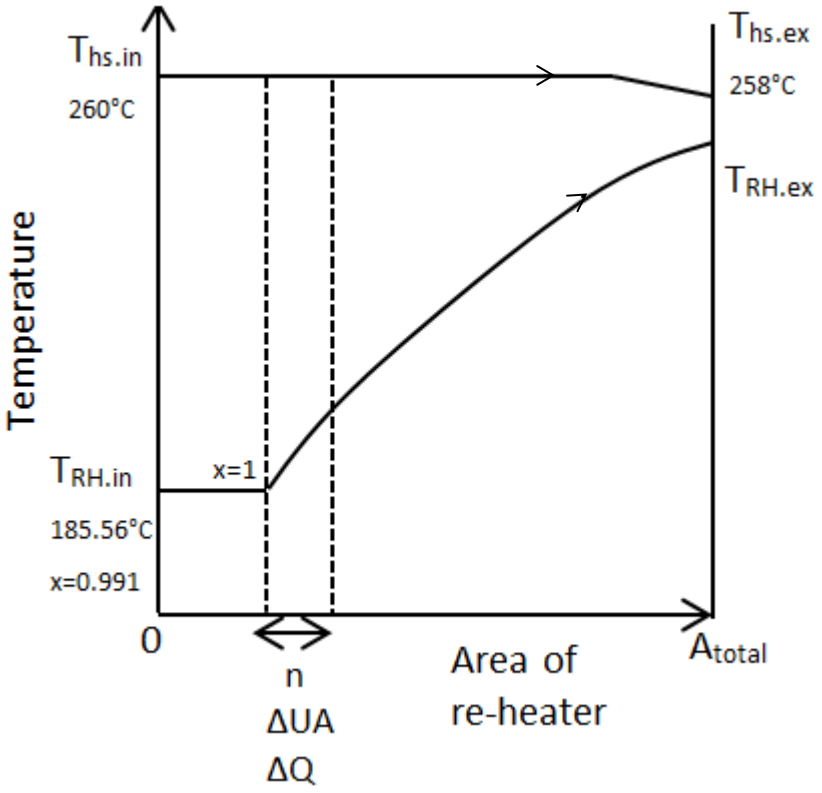

Figure 22: Condensing heat exchanger temperature profile with phase change and sub-cooling of the heating steam

To model the reheater, the reheater total heat transfer is calculated using the heating steam design properties.

Figure 22 shows the expected heat exchanger temperature profile for a condensing heat exchanger, where there is evaporation and superheating of the cycle steam. The heat exchanger can be visually separated into two parts i.e. evaporating and superheating. The dip at the end of the heating steam profile is due to sub-cooling where the condensate is slightly cooled to below saturation to avoid flashing. In this study however, sub-cooling will not be considered.

UA can be estimated using the LMTD method. A reheater discretisation method is used to determine the temperature, enthalpy, and heat transfer profiles of the steam through the reheater. The total heat transfer calculated from the discretisation method is compared to the initial heat transfer calculation, and UA is calibrated to achieve a heat transfer output close to the initial design calculation. This calibration allows for a more correct heat transfer input into the discretisation calculation and more accurate reheater temperature and enthalpy profiles. The MSR outputs, as calculated by the model, are then validated against manufacturer specifications.

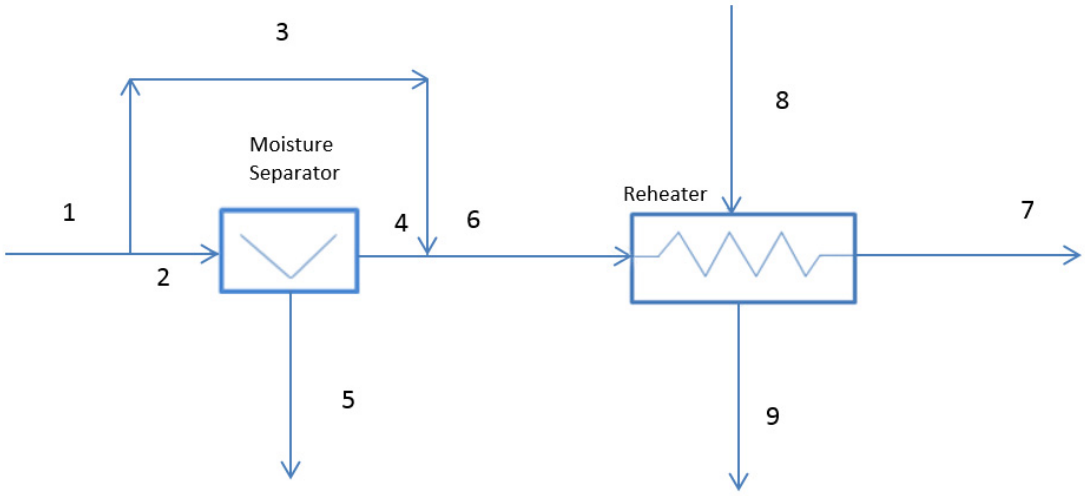

Figure 23: Schematic of the moisture separator reheater streams used in model

1 - High-pressure turbine exit
2 - Moisture separator inlet
3 - By-pass
4 - Moisture separator exit
5 - Condensate exit
6 - Reheater inlet
7 - Reheater exit steam
8 - Heating steam inlet
9 - Heating steam exit

The numbered streams above are used as subscripts for the associated variables in the following calculations.

Table 1: Known steam properties for MSR inlet and exit, obtained from manufacturer specifications

Steam property	Symbol used
MSR inlet flow rate	$\dot{m}_1$
MSR inlet steam quality	x_1
Reheater inlet mass flow rate	$\dot{m}_6$
Reheater inlet pressure	P_6
MSR exit pressure	P_7
MSR exit temperature	T_7
MSR exit enthalpy	h_7
Heating steam exit temperature	T_9
Heating steam exit enthalpy	h_9
Heating steam inlet pressure	P_8
Heating steam inlet temperature	T_8
Heating steam inlet enthalpy	h_8
Heating steam inlet pressure	P_8
Heating steam inlet quality	x_8
Heating steam inlet mass flow rate	$\dot{m}_8$
Heating steam exit pressure	P_9

The moisture separator exit quality, x_4, is determined as a function of the separator inlet quality and mass flow rate as well as the reheater inlet mass flow rate.

$$x_4 = \frac{\dot{m}_1 x_1}{\dot{m}_4} \qquad 4\text{-}1$$

The reheater total heat transfer, Q_{total}, is calculated in Equation 4-2 using the enthalpy and mass flow of the heating steam.

$$Q_{total} = \dot{m}_8(h_8 - h_9) \qquad 4\text{-}2$$

In Equation 4-3 the reheater inlet enthalpy is calculated as a function of the reheater inlet mass flow, exit enthalpy and the total heat transfer. The reheater inlet enthalpy is required as an input into Equation 4-6 as 'h_{6i}' for the first reheater section. Steam Tables is used to determine the reheater inlet temperature, T_6, for the corresponding enthalpy and pressure.

$$h_6 = h_7 - \frac{Q_{total}}{\dot{m}_6} \qquad 4\text{-}3$$

The product of the overall heat transfer coefficient and the heat transfer area, UA, is assumed to be constant. This assumption is based on the heat exchanger area remaining constant as well as the overall heat transfer coefficient, U, not impacted by changes in mass flow velocities.

U for the shell side of the condensing heat exchanger is not a function of mass flow but it is a function of temperature differences between the fluid and the vapor. As explained in Chapter 2 the dominant driver for the shell side calculation for U in a condensing heat exchanger is the temperature gradient between tube and shell side. Although the vapor mass flow changes as conditions in the moisture separator changes, the heat exchanger inlet temperatures stay about the same with negligible variances. The tube side is not affected because the velocities therein remain constant. As both the inside and outside heat transfer coefficient is not expected to change substantially, it is safe to assume that U remains constant. It is acknowledge that this assumption will not be accurate for the initial plateau part of the heat transfer profile, however this is a small part of the overall process and therefore the error made should not be significant.

UA is calculated as an initial estimate, using Q_{total}, from Equation 4-2 and the log mean temperature, calculated using Equation 2-1.

Initial estimate UA:

$$UA = \frac{Q_{total}}{\Delta T_{lm}} \qquad 4\text{-}4$$

The initial estimate UA is later calibrated with correction factor, C_F. The correction factor is introduced to give a more accurate heat transfer rate, which is an input into the calculation of the reheater temperature and enthalpy profiles. This is needed as the log mean temperature calculation for heat transfer assumes that the temperature and steam flow properties are uniform over every flow cross-section. This is not accurate for a reheater with discernible zones of different temperature gradients i.e. constant temperature where excess moisture in the steam is being evaporated followed by an increase in temperature where the steam is superheated.

It is not known where the changes in these zones are, i.e. where the change is from saturation to super-heating, and therefore to determine the actual temperature profile, the reheater is split into very small sections. Each section is separately analysed to approach an integral solution in the model.

The reheater temperature profile in Figure 22 represents the discretisation method where ΔUA is the UA per reheater section, i.e.$\Delta \mathrm{UA} = \frac{\mathrm{UA}}{\mathrm{n}}$, and 'n' is the total number of reheater sections.

ΔUA is assumed to be constant for every reheater section and does not change with flow or operating conditions. This assumption is a simplification used as, unless the actual heat transfer coefficient per section is calculated, this approach is the only feasible method for the scope of this study.

For the purpose of this study it is also assumed that there is no sub-cooling of the heating steam condensate. In sub-cooling there is a small amount of heat transfer which does not warrant the complexity of the calculation required to quantify it.

Discretisation methodology

The discretisation method involves sectioning the steam flow path through the reheater into a number of sections, n and iteratively calculating the temperature, enthalpy, and heat transfer per section to enable an accurate plot of the profiles of the steam through the heat exchanger. The number of sections chosen determines how 'fine' or 'coarse' the calculation will be. If the number of sections is too few the profile will be too coarse and the change in reheater zones could be missed. A number too large might result in excessive and redundant calculations. A sensitivity analysis is required to assist in selecting the number of reheater sections.

Discretisation sensitivity analysis

To select the total number of sections, 'n', to divide the reheater into, a sensitivity analysis is used. For the analysis, a random range of 'n' is chosen i.e. 20 to 5 200. The overall heat transfer is calculated for every value of 'n' in that range. The heat transfer per 'total number of sections' from 20 to 5200 is plotted. When the plotted curve plateaus, it demonstrates model insensitivity over the plateaued range of sections. The sensitivity analysis is important to ensure that the increments chosen are not too few; however there is no penalty in choosing a large number of increments as this model solves within a few seconds on a normal PC. The 'n' value selected, which is within the plateau of Figure 24, is 4800, though a number 2000 might have been just as adequate.

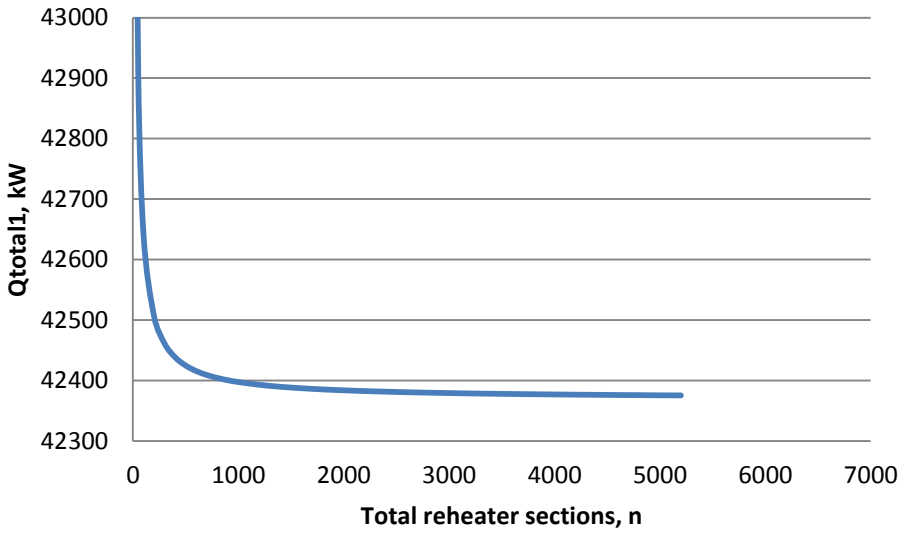

Figure 24: Discretisation sensitivity curve

Discretisation algorithm

An iterative loop is applied over the total number of sections to determine the reheater heat transfer, temperature, and enthalpy profiles as well as exit conditions. The total heat transfer can be obtained by adding the calculated heat transfer of each individual section. The loop is based on the following two equations:

$$\Delta Q_i = \Delta UA(T_8 - T_{6i}) \qquad 4\text{-}5$$

Where:

- ΔQ_i = heat transfer for section i, kW
- ΔUA = heat transfer coefficient × area, per reheater section, kW/K
- T_8 = heating steam inlet temperature, K
- T_{6i} = reheated steam inlet temperature for section i, K

$$h_{6_{i+1}} = \left(\frac{\Delta Q_i}{\dot{m}_6}\right) + h_{6_i} \qquad 4\text{-}6$$

Where:

- h_{6i} = reheater inlet enthalpy for section i, kJ/kg
- h_{6i+1} = reheater exit enthalpy for section i, kJ/kg
- $\dot{m}_6$ = reheater mass flow rate, kg/s

These equations are used for each reheater section. The heat transfer for the first section is calculated using Equation 4-5. The reheater inlet steam temperature, T_6, is

determined from Steam Tables for the corresponding pressure and reheater inlet enthalpy (from Equation 4-3).

The calculated heat transfer from Equation 4-5 and the reheater inlet enthalpy from Equation 4-3 are inputs into Equation 4-6 to calculate the exit enthalpy for the first reheater section. The corresponding exit temperature is determined via Steam Tables. The calculated exit steam properties (temperature and enthalpy) become the inlet steam properties for the next section and are used again in Equations 4-5 and 4-6. ΔUA remains constant. The calculations are iterated over the number of sections selected.

$$\begin{aligned}&\text{for}\quad i \in 0..n\\ &\left\|\begin{aligned}&h_{i+1} \leftarrow h_i + \frac{\Delta Q_i}{\dot{m}_6}\\ &T_{i+1} \leftarrow T_{steam}\left(P_6, h_{i+1}\right)\\ &\Delta Q_{i+1} \leftarrow \Delta UA \cdot \left(T_8 - T_{i+1}\right)\end{aligned}\right.\end{aligned}$$

Figure 25: Algorithm developed for the iterative computation of reheater outputs in increments, i calculated over total number of sections, n.

The discretisation algorithm in Figure 25 produces the reheater temperature, enthalpy and heat transfer profiles. The total heat transfer, Q_{total1}, which is the sum of the heat transfer per individual reheater section, is calculated using Equation 4-7. The model outcomes of the reheater temperature, enthalpy and heat transfer profiles for design conditions can be seen in Figures 26, 27 and 28.

$$Q_{total1} = \sum_{i=1}^{n} \Delta Q_i \qquad 4\text{-}7$$

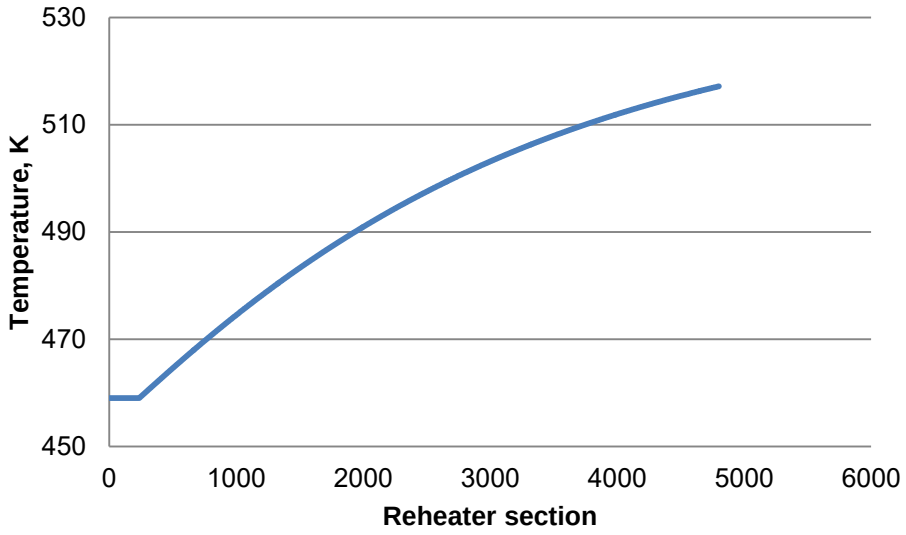

Figure 26: Temperature profile over number of reheater sections

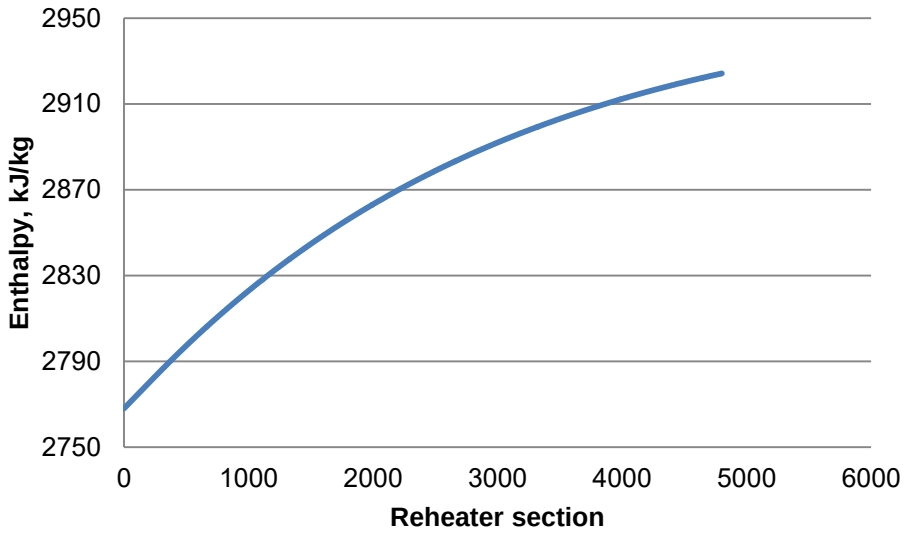

Figure 27: Enthalpy profile over number of reheater sections

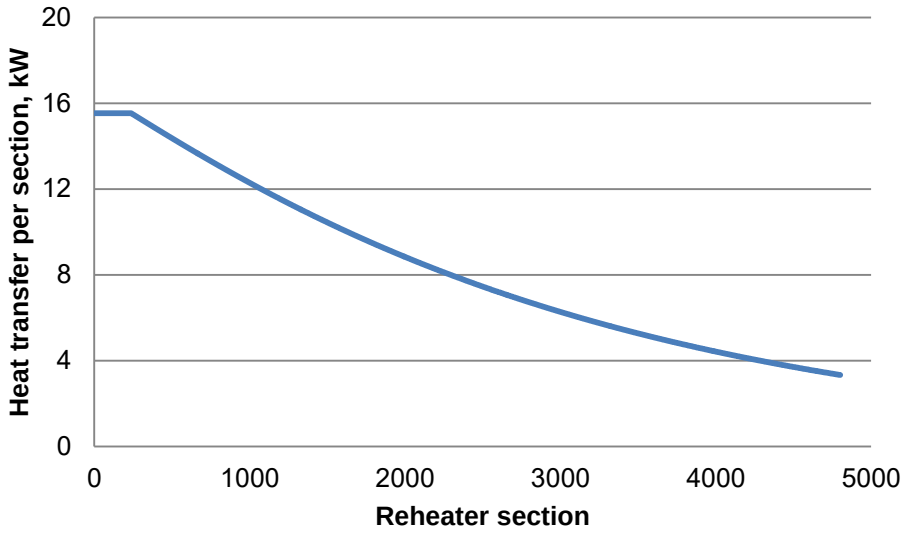

Figure 28: Heat transfer profile over number of reheater sections

Calibration

The correction factor, C_F, is used to calibrate the initial estimate UA. This determines ΔUA, which is an input into Equation 4-5 and the reheater discretisation algorithm. The calibration aims to adjust UA so that the overall heat transfer determined from the model, Q_{total1}, is within a range of less than 0,1% difference to Q_{total}, which was calculated using manufacturer specifications for the heating steam properties, in Equation 4-2.

Table 2: Initial heat transfer calculated vs calibrated heat transfer

Initial estimate UA x 10^3 kW/K	Calibrated UA x10^3 kW/K	C_F	Q_{total} kW	Q_{total1} kW
1,131	1,008	0,891	40 600	40 604

$$\frac{Q_{total1} - Q_{total}}{Q_{total}} = 0.009\% \qquad 4\text{-}8$$

Reheater Performance

The performance of the reheater is characterised in this study using the terminal temperature difference (TTD). The reheater TTD is equal to the heating steam saturation temperature (at the operating pressure) minus the reheater outlet steam temperature. TTD provides feedback on the performance of the reheater relative to heat transfer. TTD is a common metric used to measure heat exchanger performance. The lower the TTD the better the performance therefore should the TTD change from a lower to a higher value it gets interpreted as a poorer performing heat exchanger. [25]

Steam consumption is also used as a measure of performance as the more steam consumed by the process the less steam is available for electricity production. Excessive amounts of steam consumption is due to additional liquid being required to be heated therefore the result is that the system becomes less efficient.

The TTD and mass steam consumption for this design is calculated using Equations 4-9 and 4-10 respectively. The TTD calculated for design conditions is 16,01 K.

$$\mathrm{TTD} = \mathrm{T_{8sat}} - \mathrm{T_7} \qquad 4\text{-}9$$

$$\text{steam consumption} = \frac{\mathrm{Q_{total1}}}{\mathrm{h_8} - \mathrm{h_9}} \qquad 4\text{-}10$$

Validation of model outcomes

The model is used to calculate the reheater exit temperature and enthalpy for design conditions. These outcomes are validated by comparing them to the manufacturer specifications. The model outcomes show a marginal percentage deviation, when compared to the manufacturer specifications.

In Table 3 it can be seen that there is a positive difference between the TTD given by the manufacturer and the TTD determined with the model. This difference is due to the small sub-cooling which occurs in the actual reheater. For the purpose of the study however, sub-cooling was disregarded.

Table 3: Model outcomes for MSR exit conditions vs manufacturer specifications

	Model	Manufacturer specifications	% deviation
Reheater exit temperature, T_7	517,141 K	516,68 K	– 0,89
Reheater exit enthalpy, h_7	2 924,18 kJ/kg	2 924,21 kJ/kg	0,0012
TTD	16,01	16,42	2,5

4.2 Modelling the selected moisture separator defects

The most significant performance parameters for a moisture separator are removal efficiency and pressure differential. These two degradation conditions both have an impact on the steam velocity through the moisture separator. Steam velocity is an input into the equations defining the separator removal efficiency and pressure differential. Separator removal efficiency and pressure differential affect steam properties such as temperature and enthalpy, which in turn, affect the reheater profiles for temperature, enthalpy and heat transfer as well as MSR performance. The model integrates this causal relationship via a series of relating equations and calculations.

The two degradation conditions included into the MSR model are:

- Fouling of the moisture separator vane channels resulting in blockage.
- Material deterioration of the separator vanes resulting in steam bypass of the moisture separator.

The blockage defect impacts the amount of available separator surface area and the bypass defect impacts the remaining steam mass flow rate through the separator. Area and mass flow rate are functions of steam velocity as defined by Equation 4-11.

$$v_2 = \frac{\dot{m}_2}{\rho_g A_2} \qquad 4\text{-}11$$

This calculated velocity is an input into Equation 3-1 to determine pressure drop, and Equation 3-2 for separator vane efficiency.

Moisture separator pressure differential

Pressure differential across the moisture separator vanes is impacted by flow dynamics through the vane as defined by separator vane dimensions and steam properties such as density and velocity. The relationship between these properties is represented in Equation 3-1 [23]. Separator vane data was obtained from manufacturer specifications, constants from engineering data on flow of fluids and steam properties were extracted from Steam Tables.

Moisture separator removal efficiency

Equation 3-2 [24] for droplet removal efficiency provides insight into factors that affect separator efficiency, one of which is gas velocity. The moisture separator geometric parameters are obtained from the manufacturer specifications, i.e. number of bends, spacing between plates, and angle of bend. The droplet density and the dynamic viscosity are extracted from Steam Tables for the associated inlet pressure, temperature, and enthalpy.

Droplet size is an input into Equation 3-2. Before the droplet removal efficiency can be calculated, Equation 3-2 is first used to calibrate the droplet size for the required separator efficiency under design conditions. For a moisture separator exit steam quality of 0,991, obtained from Equation 3-2, the corresponding droplet size is $4{,}2 \times 10^{-5}$ m.

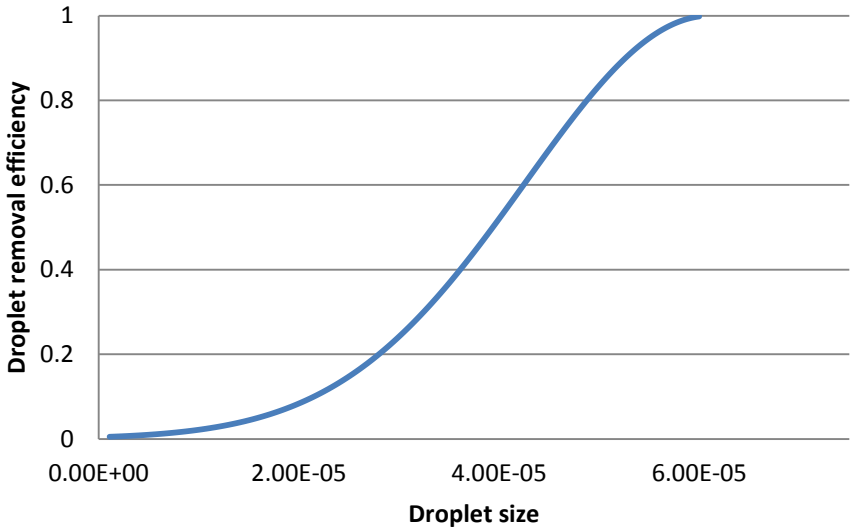

Figure 29: Moisture removal efficiency vs. droplet size

It can be seen from Figure 29 that for smaller droplet sizes the moisture removal efficiency decreases which is explained by smaller droplets having less momentum and being less prone to inertia and therefore less susceptible to the moisture removal mechanism of inertial impingement. The droplet removal efficiency calculated applies to the removal of droplets of the determined size, $4{,}2 \times 10^{-5}$ m and larger.

4.2.1 Blockage of separator vanes

To determine the impact of the blockage of an area of separator vane channels, the simulated blocked area is subtracted from the total moisture separator surface area and the new area is used to calculate velocity through the separator using Equation 4-11. The changed velocity is an input into Equations 3-1 and 3-2 respectively, to determine the impact on pressure differential and separator vane efficiency.

The moisture separator vane efficiency is then used to calculate the separator exit steam quality. Steam enters the moisture separator at a certain quality. Steam quality is the proportion of saturated steam (vapour) in a saturated condensate (liquid)/ steam (vapour) mixture. A steam quality of 0 indicates 100 % liquid, (condensate) while a steam quality of 1 indicates 100 % steam. The separator vane efficiency is the ability to remove a fraction of the water vapour droplets. To calculate the moisture separator exit steam quality, the vane efficiency is applied to the mass of droplets in the inlet steam to determine the mass of water removed. The remaining mass of droplets is added to the inlet dry steam to calculate the total exit steam quality.

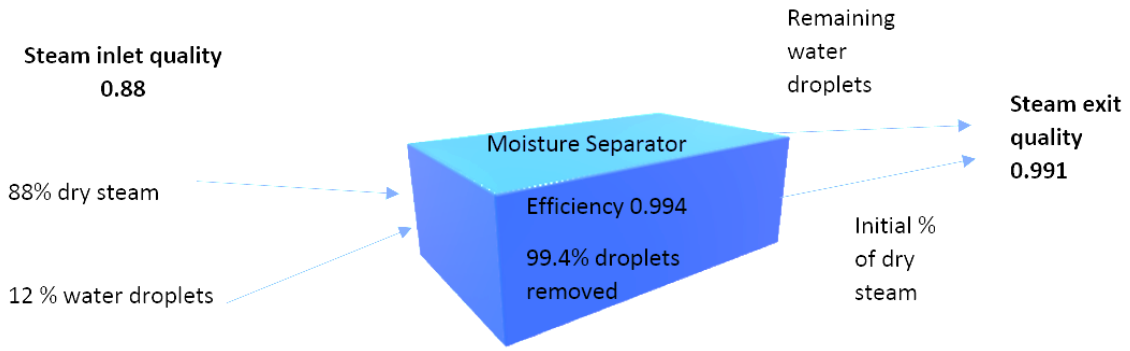

Figure 30: Schematic of separator exit steam quality calculation

Figure 30 and Equation 3-2 represent the calculation for moisture separator exit steam quality, where the vane efficiency $\eta_{(d_d)}$ is applied to the mass of inlet water droplets to determine the mass of water removed. The ratio of the remaining water droplet mass against the inlet dry steam mass is used to calculate the moisture separator exit steam quality.

Equation 4-12 is derived in the following manner:

Vapour content in stream 2, $\dot{m}_{V2} = x_2 \dot{m}_2$

Liquid content in stream 2, $\dot{m}_{L2} = \dot{m}_2(1 - x_2)$

Water content in stream 4, $\dot{m}_{L4} = \dot{m}_2(1 - x_2) - \eta_{(d_d)}[m_2(1 - x_2)]$

Vapour content in stream 4, $\dot{m}_{V4} = \dot{m}_4 - \dot{m}_{L4}$

$$= \dot{m}_4 - \left[(1 - \eta_{(d_d)})m_2(1 - x_2)\right]$$

Given that steam quality is the proportion of saturated steam vapour in a saturated condensate/steam vapour mixture:

$$x_4 = \frac{\dot{m}_{V4}}{\dot{m}_4}$$

$$x_4 = \frac{\dot{m}_4 - \left[(\eta_{(d_d)})\dot{m}_2(1 - x_2)\right]}{\dot{m}_4}$$

$$x_4 = 1 - \left[\frac{\dot{m}_2(1 - x_2)(1 - \eta_{(d_d)})}{\dot{m}_4}\right] \qquad 4\text{-}12$$

The separator exit quality and pressure is used to extract the corresponding enthalpy and temperature values from Steam Tables, which are the inputs into Equations 4-5 and 4-6 in the iterative loop in Figure 25, to calculate reheater exit conditions.

4.2.2 Bypass of separator

To mathematically represent moisture separator bypass, a percentage mass flow of steam, $\dot{m}_3$, is assumed to bypass the separator vanes, leaving less flow through the moisture separator. The bypass steam is not treated through the separator and mixes with the steam exiting the vanes to give a certain steam quality at the reheater inlet. The steam flowing through the separator does so at a reduced velocity as calculated by Equation 4-11. This velocity is inputted into Equations 3-1 and 3-2 to determine the separator exit pressure and efficiency respectively. The steam quality and pressure at the separator exit is used, with Steam Tables, to obtain the associated enthalpy, h_4, which is an input into Equation 4-13. A mass flow rate balance is used to calculate $\dot{m}_4$.

The mixing calculation in Equation 4-13 is used to determine the reheater inlet enthalpy, h_6, after which the corresponding steam temperature, at the reheater inlet pressure, is obtained using Steam Tables.

$$h_6 = \frac{\dot{m}_3 h_3 + \dot{m}_4 h_4}{\dot{m}_6} \qquad 4\text{-}13$$

It is assumed that the total surface area of the separator vanes remains unchanged by the deterioration. As a result, the velocity inside the separator drops as more steam flow bypasses the moisture separator. This is a simplification, but the alternative would be to quantify the mass flow balance based on a specific size of the bypass hole, which in turn would require assumptions on the pressure drop characteristics of the hole. This is beyond the scope of the study.

The calculated reheater inlet enthalpy and corresponding temperature are inputs into Equations 4-5 and 4-6 in the iterative loop, used to calculate reheater exit conditions.

5 Results and analysis

The results demonstrated the effect of blockage and bypass of the moisture separator on the MSR exit steam properties and performance. The model mathematically demonstrated the impact that separator degradation has on the droplet removal efficiency and pressure drop of the moisture separator, and the consequent effect on other MSR steam properties and performance.

5.1 Blockage of moisture separator channels

The blockage of a percentage surface area of the moisture separator vane channels was simulated. The blockage reduced the moisture separator area through which the steam flows. In Table 4, as the blocked area increases, the velocity through the vane channels increases, while the pressure of the steam exiting the moisture separator decreases. In addition, the reheater steam properties are observed to improve with an increase in separator blockage. The simulation was run up and until a separator steam exit quality of 1 was reached, which corresponds to a separator area blockage of 56 percent, as shown in Table 4. All results in this chapter are therefore presented for the range of 0 to 56 percent blockage.

Table 4: Results for percentage of blocked vane channels

% blocked	v m/s	P_4 bar	x_4	h_6 kJ/kg	T_6 K	Q_{total1} kW	T_7 K	TTD K	steam consumption kg/s
0	2,58	11,37	0,991	2 762,98	458,71	41 561,76	516,81	16,34	24,94
8	2,81	11,36	0,993	2 766,91	458,65	40 868,42	517,09	16,06	24,52
14	**3.01**	**11.35**	**0.994**	**2769.51**	**458.6**	**40316.29**	**517.37**	**15.78**	**24.19**
16	3,08	11,34	0,994	2 770,34	458,58	40 140,94	517,45	15,70	24,08
24	3,41	11,32	0,996	2 773,42	458,49	39 493,29	517,77	15,38	23,70
32	3,81	11,29	0,997	2 776,04	458,36	38 951,82	518,04	15,11	23,37
40	4,31	11,24	0,998	2 778,10	458,17	38 545,31	518,24	14,91	23,13
48	4,98	11,17	0,999	2 779,50	457,89	38 303,99	518,38	14,77	22,98
56	5,88	11,01	1	2 780,16	457,45	38 261,09	518,44	14,71	22,96

5.1.1 Impact on moisture separator parameters

The blocked vane channels reduce the area left for moisture separation to take place. This reduced area needs to accommodate the same mass flow rate of steam, which results in an increased velocity and pressure drop (Table 4).

.

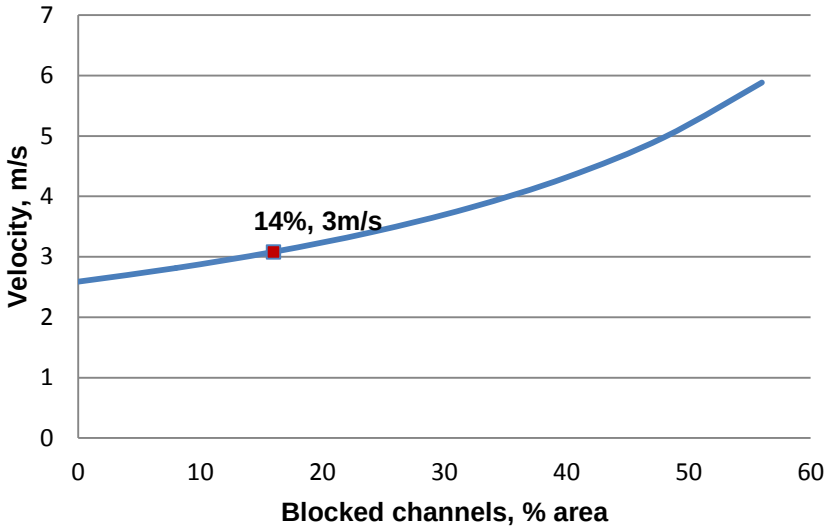

Figure 31: Velocity vs percentage blocked channels

In Figure 31 the velocity in the vane channels is observed to increase as the percentage of blocked channels increases. As the velocity of steam increases, the separation mechanism of inertial impingement is more effective due to more water droplets impinging on the vane surface as a result of their increased momentum reducing the ability of the droplets to change direction with the channel wave-like configuration. As more water droplets are removed from the steam, the moisture separator exit steam quality increases with an increase in the separator blocked area (Figure 32). The steam quality increases until an upper velocity limit is reached due to re-entrainment.

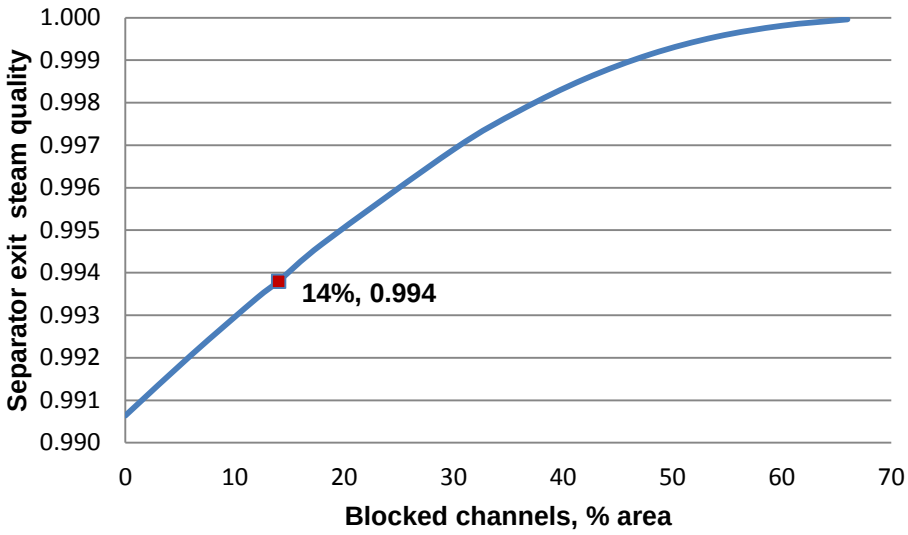

Figure 32: Separator exit steam quality vs percentage blocked channels

Critical velocity for re-entrainment

The maximum critical velocity above which re-entrainment of water droplets back into the steam flow takes place is calculated, using Equation 3-3, as 3m/s.

Table 4 and Figure 31 show that this limit is reached at 14 percent blocked channels with a corresponding steam exit quality of 0,994 (Figure 32). The model however shows a continued improvement in moisture separator steam exit quality as the steam velocity increases above 3 m/s. A steam quality of 1, saturated steam is theoretically reached at a separator velocity of 5,88 m/s and 56 percent blockage. However, literature explains that above the critical velocity, droplets that have been entrained onto the blades are swept up in the high-speed flow and re-entrained back into the steam flow.

Practically, this would negate any theoretical improvement in moisture separator efficiency as the exit steam quality will deteriorate. It can be assumed that, above 14% blockage, the separator exit steam quality does not necessarily improve as the model indicates, and that the maximum efficiency, with an exit steam quality of 0.994, is most likely achieved at 14 percent blockage.

Pressure drop

The increase in velocity affects the pressure drop across the moisture separator as well as the temperature of steam exiting the moisture separator, and then entering the reheater.

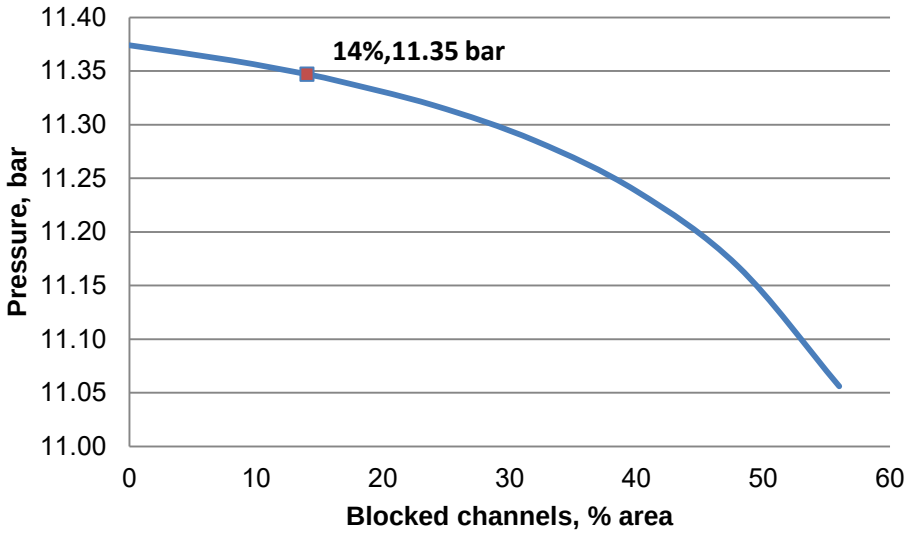

Figure 33: Moisture separator exit pressure vs percentage blocked channels

As the percentage of blocked vane channels increases, the moisture separator exit pressure is observed, in Figure 33, to decrease. The greater pressure drop over the moisture separator is attributed to the increase in velocity as the channels are blocked.

Pressure and temperature are directly proportional in saturated steam, as seen in Figures 33 and 34. As the pressure decreases, the temperature decreases.

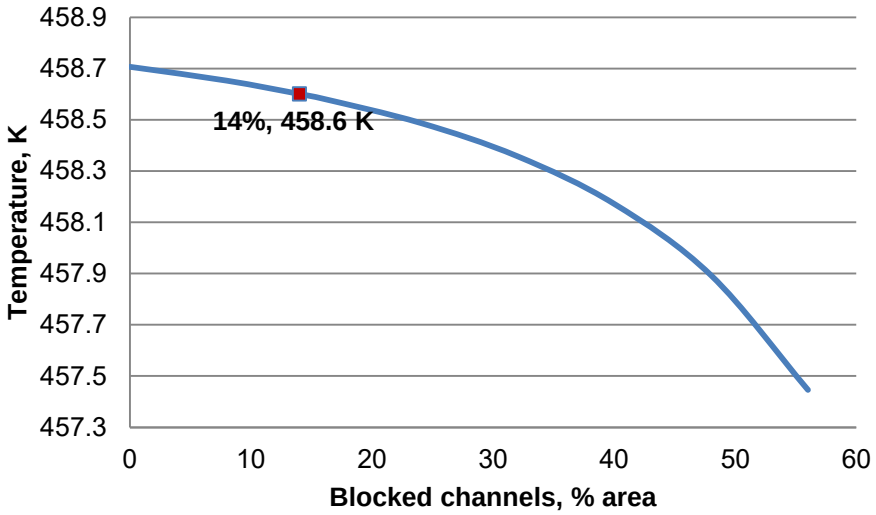

Figure 34: Moisture separator exit temperature vs percentage blocked channels

5.1.2 Impact on reheater steam properties

The quality of steam at the moisture separator exit improves with the increase in blocked channels, as seen in Figure 32. The increase in enthalpy as seen in Figure 35 can be explained by the improved steam quality. As water in vapour phase has a much higher enthalpy than in the liquid phase, steam with a low liquid content would therefore have a higher enthalpy than steam with a higher liquid content. Note that this is only valid up to the critical blocked channel percentage of 14 percent.

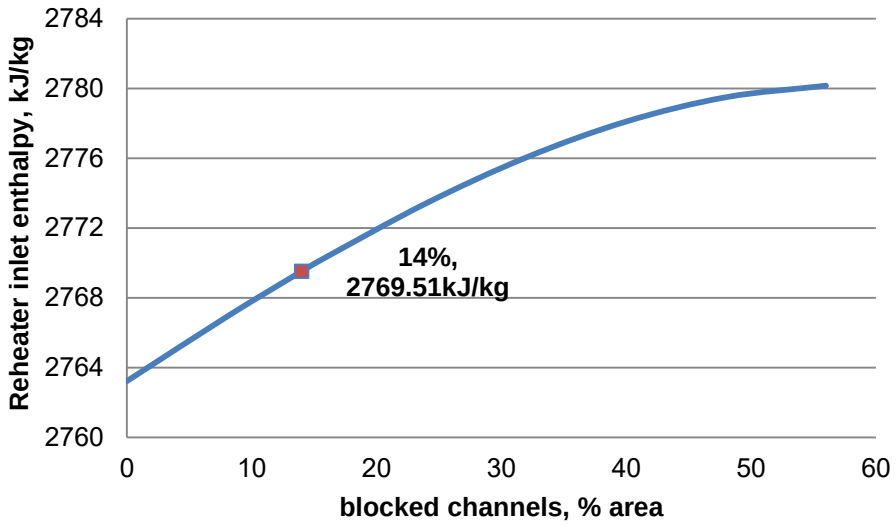

Figure 35: Reheater inlet enthalpy vs percentage blocked channels

As the blocked area increases up to 14 percent and there is an improvement in reheater inlet steam quality, less heating steam is required for the latent heat transfer for evaporation of water droplets, leaving more heating capability available to further increase the temperature of the steam. This results in the increase of reheater exit temperatures as the area of blocked channels increases, as seen in Figure 36.

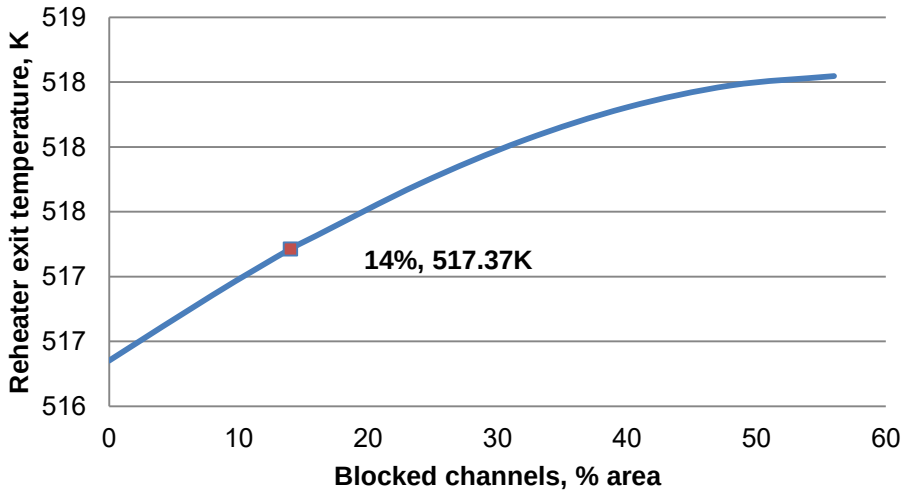

Figure 36: Reheater exit temperature vs percentage blocked channels

5.1.3 Impact on reheater temperature profiles

In Figure 37 the reheater temperature profiles are compared between 0, 20 and 40 percent blockage in the separator. For no blockages, the temperature remains unchanged from n = 0 to n = 310. During phase change of the water droplets in the steam, the steam temperature does not increase and is represented in the graph as a plateau. After all water droplets have been evaporated the temperature of the steam steadily increases. For a 20 percent blockage, the temperature remains unchanged until n = 162 and for 40 percent it remains unchanged until n = 54, after which it steadily increases. As the blockage area increases the quality of steam at the reheater inlet improves, consequently there is less water in the steam and therefore less heat required for latent heat transfer (evaporation) prior to sensible heat transfer (superheating), as the shorter plateaued temperature range with increased percentage blockage shows. This results in the steam exiting the reheater at a higher degree of superheat. The reheater exit temperature for 40 percent blockage is therefore higher than for 0 and 20 percent blockage.

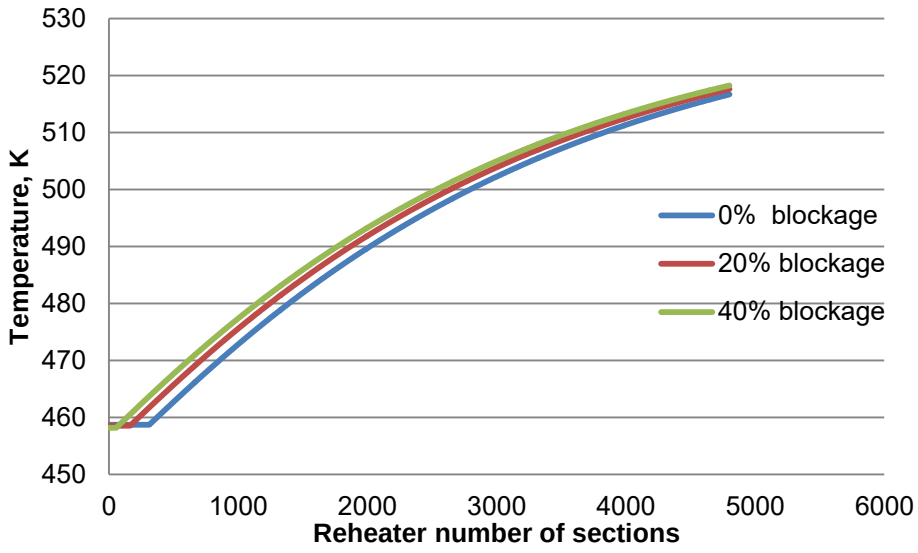

Figure 37: Reheater temperature profiles for 0%, 20% and 40% separator blockage

5.1.4 Impact on MSR performance

The area of blocked moisture separator vane channels affects the reheater exit temperature which impacts the measured MSR performance as characterised by TTD.

The TTD improves as the blockage increases, up to a blockage that corresponds to the critical velocity of 3.0 m/s, see Figure 38. This is primarily due to the separator blockage resulting in a higher degree of superheat achieved as seen in Figure 37. As a higher degree of superheat is achieved, it reflects in a reduced delta between the

cycle steam and the heating steam saturation temperature resulting in the improved TTD.

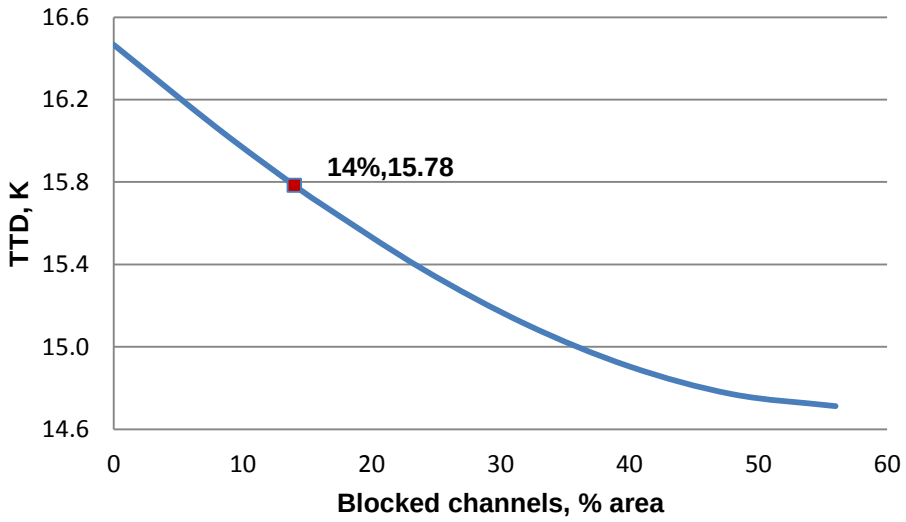

Figure 38: TTD vs percentage blocked channels

The decrease in heating steam consumption, see Figure 39, further supports this where less steam is consumed as the area of blocked channels increases. The decrease in heating steam consumption is due to less moisture in the steam and therefore less heating steam required for latent heat transfer, before the steam can be superheated. The mechanism to draw more steam is due to the larger average temperature difference for the case with a large amount of moisture, as the region where evaporation occurs is bigger.

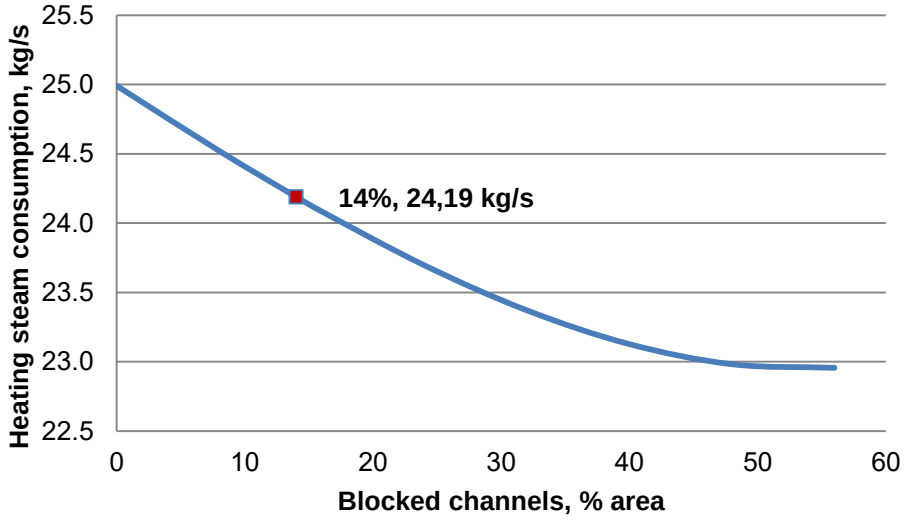

Figure 39: Heating steam consumption vs percentage blocked separator channels

Similarly Figure 40 shows that as the percentage of blocked vanes in the moisture separator increases, the total heat transferred over the reheater decreases, i.e. less heat is required to evaporate and then superheat the steam. Note that this is only valid up to the critical blocked channel percentage of 14 percent.

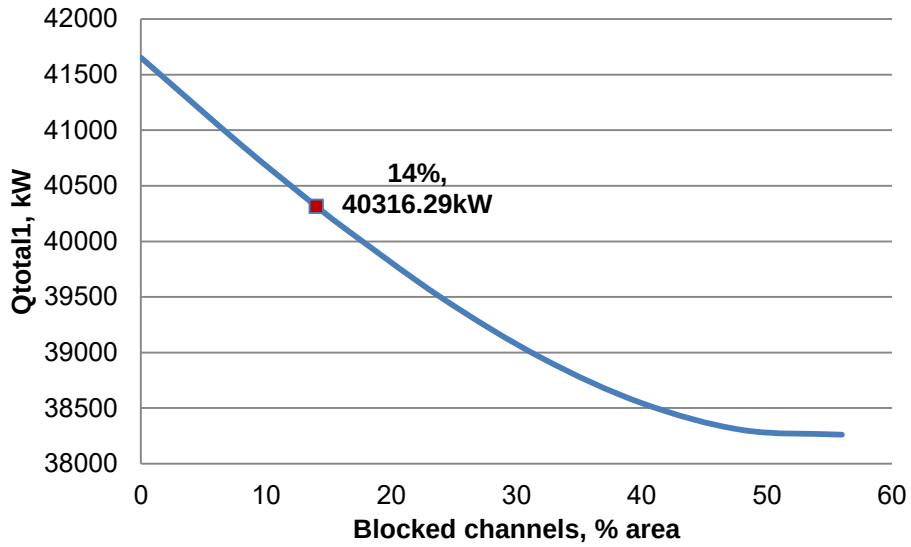

Figure 40: Total reheater heat transfer vs percentage blocked separator channels

5.2 Bypass of moisture separator

Material deterioration of the separator vanes causing a steam bypass of the moisture separator was simulated. This bypass steam does not alter in moisture content as it passes through the vessel. It then mixes with the cycle steam exiting the moisture separator vanes, after which the mixture enters the reheater at a certain quality and enthalpy.

The bypass flow is calculated as a percentage of the steam mass flow at the moisture separator inlet which has been diverted to the bypass stream; however, it is assumed that the loss in moisture separator area due to separator vane deterioration is negligible.

Table 5: Results for percentage of bypass flow

% bypass	v m/s	P_4 bar	x_4	h_4 kJ/kg	h_6 kJ/kg	x_6	Q_{total1} kW	T_7 K	TTD K	steam consumption kg/s
0	2,58	11,37	0,991	2 763,21	2 763,21	0,991	41 652,72	516,68	16,47	24,99
10	2,33	11,38	0,988	2 757,81	2 735,89	0,977	47 432,52	513,37	19,78	28,46
20	2,07	11,40	0,984	2 750,83	2 709,13	0,963	52 855,90	509,49	23,66	31,71
30	1,81	11,41	0,98	2 741,85	2 683,05	0,95	57 831,34	505	28,15	34,7
40	1,55	11,42	0,974	2 730,31	2 657,85	0,938	62 256,31	499,9	33,25	37,35
50	1,29	11,43	0,967	2 715,55	2 633,85	0,926	66 026,32	494,24	38,91	39,61
60	1,03	11,43	0,957	2 696,74	2 611,54	0,914	69 052,04	488,21	44,94	41,43
70	0,77	11,44	0,945	2 672,90	2 591,60	0,904	71 284,80	482,13	51,02	42,77
80	0,51	11,44	0,93	2 642,87	2 575,06	0,898	72 745,15	476,58	56,57	43,65
90	0,25	11,44	0,911	2 605,34	2 563,43	0,89	73 534,74	472,4	60,75	44,12
100	0,00	11,45	0,888	2 558,90	2 558,90	0,888	73 785,34	470,71	62,44	44,27

5.2.1 Impact on moisture separator parameters

As the bypass flow increases, the reduced mass flow through the separator results in a reduced velocity and consequently reduced efficiency of the moisture separator. In Table 5 all considered parameters of the moisture separator and reheater show deterioration as the amount of steam bypass increases.

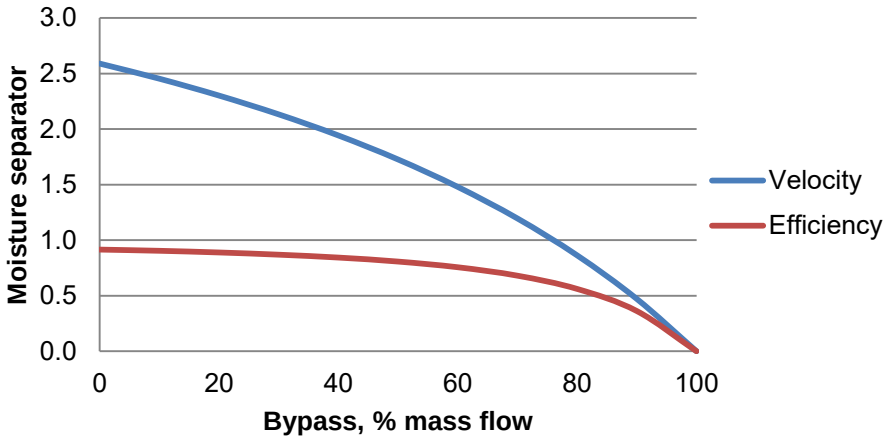

Figure 41: Percentage bypass vs moisture separator parameters

Figure 41 shows the decline in velocity of steam through the moisture separator as the percentage of steam bypass flow increases. The decline in velocity decreases the momentum of the water droplets entrained in the steam resulting in less droplet impingement on the separator vanes. The decreased removal of moisture from the process steam is reflected in the decline of the moisture separator efficiency with increased bypass.

5.2.2 Impact on reheater steam properties

The bypass steam mixes with the separator exit steam before entering the reheater. This increases the moisture content of the reheater inlet steam as noted, in Figure 43, by the decline in reheater inlet steam quality as the bypass increases.

Heat exchanger inlet specific enthalpy decreases with an increase in bypass (Figure 42). The decline in specific enthalpy can be explained by the decline in steam quality, as water in liquid phase has a much lower specific enthalpy than in the vapour phase. Steam with a high liquid content would therefore have a lower specific enthalpy than steam with a lower liquid content.

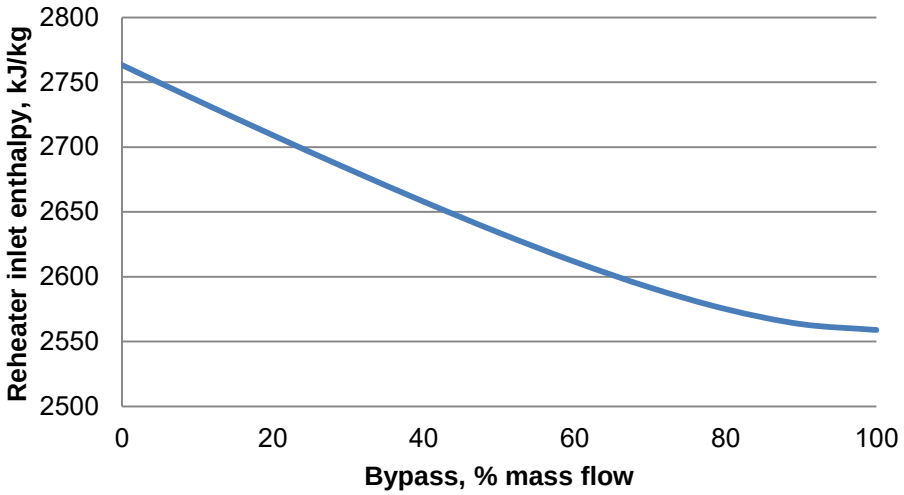

Figure 42: Reheater inlet enthalpy vs percentage bypass

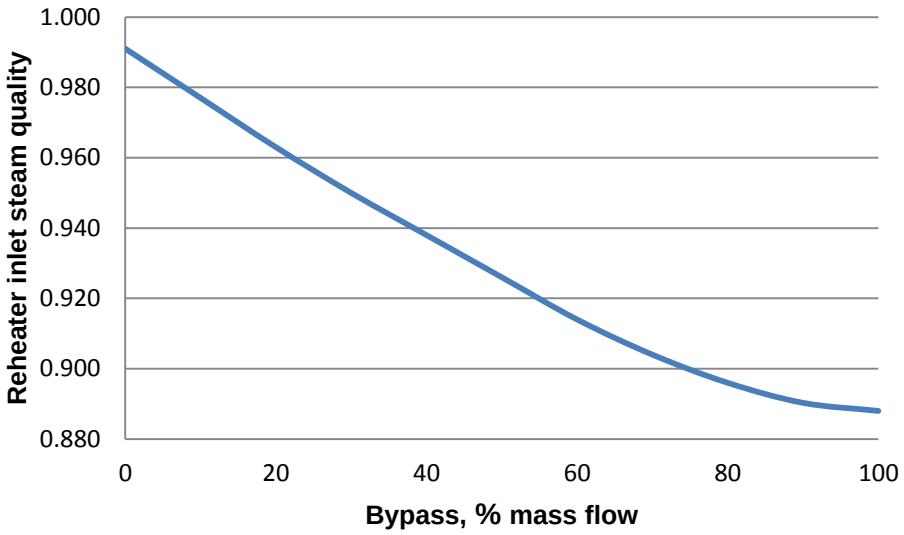

Figure 43: Reheater inlet steam quality vs percentage bypass

As the increase in bypass flow results in a deterioration of the reheater inlet steam quality, more heating steam is required for the latent heat transfer for evaporation of the water content of the steam, leaving less heat transfer capability available to further increase the temperature of the steam. This results in the decline of reheater exit temperature as the bypass increases (Figures 43, 44).

A further consequence is that the mass flow entering the reheater increases slightly due to the larger moisture content not being extracted at the separator. This further reduces the final exit temperature.

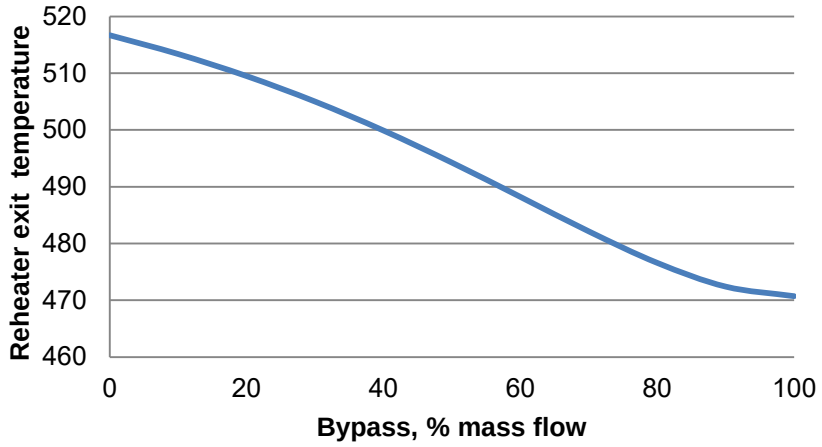

Figure 44: Reheater exit temperature vs percentage bypass

5.2.3 Impact on reheater temperature profiles

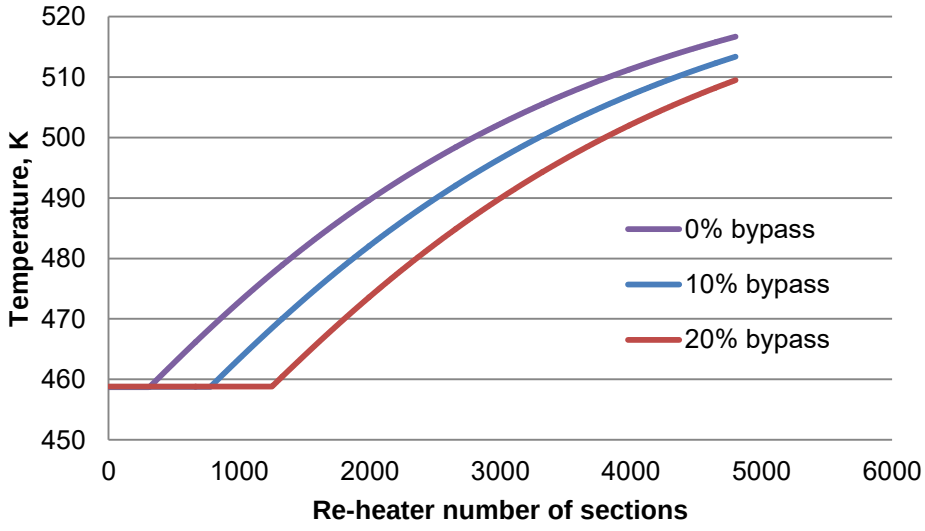

Figure 45: Reheater temperature profile at 0%, 10% and 20% bypass

An increase in bypass flow results in a deterioration of the reheater inlet steam quality, as shown in Figure 43. The effect of the increase in steam water content

entering the reheater is further reflected in the reheater temperature profiles for differing percentages of bypass flow in Figure 45. As the bypass increases the initial temperature plateau remains constant for longer due to the increased water content first being evaporated (temperature remains constant), after which the temperature increases as the steam is superheated.

The temperature profiles for 0%, 10% and 20% bypass show that as the bypass increases the reheater exit temperature decreases. As more steam bypass results in the decline in reheater inlet steam quality, an increasing amount of heat energy is required for latent heat transfer (evaporation) leaving a limited amount of heat capability left to superheat the steam.

5.2.4 Impact on MSR performance

Steam bypass of the moisture separator affects the reheater exit temperatures as seen in Figure 45, which influences the calculation of TTD.

In Figure 46, TTD increases as the bypass mass flow increases; this represents a deterioration of MSR performance. As the reheater exit temperatures decline with an increase in bypass, there is an increased delta between the cycle steam and the heating steam saturation temperature, reflected in the deterioration in MSR performance

.

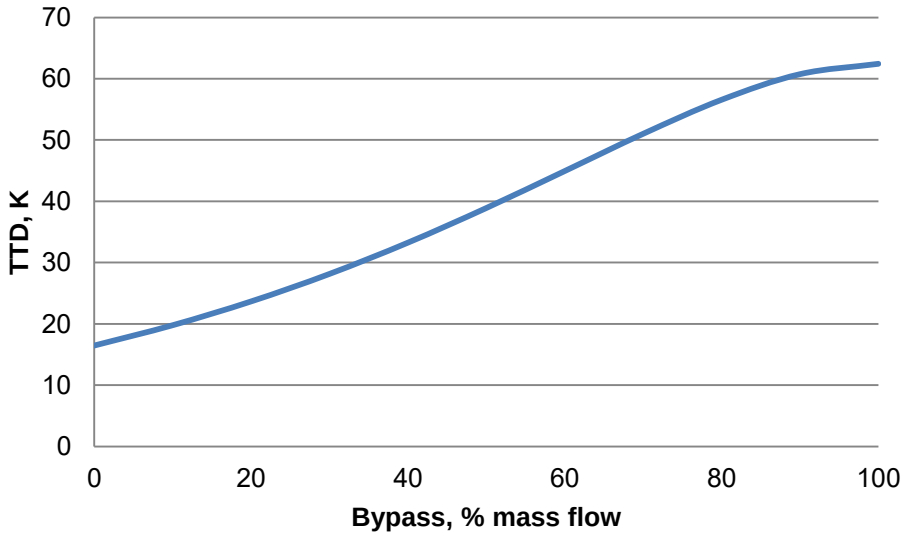

Figure 46: TTD vs percentage bypass

As more heat is required for evaporating the steam moisture content, the heating steam consumption increases, Figure 47, as well as the total heat transferred over the reheater, Figure 48.

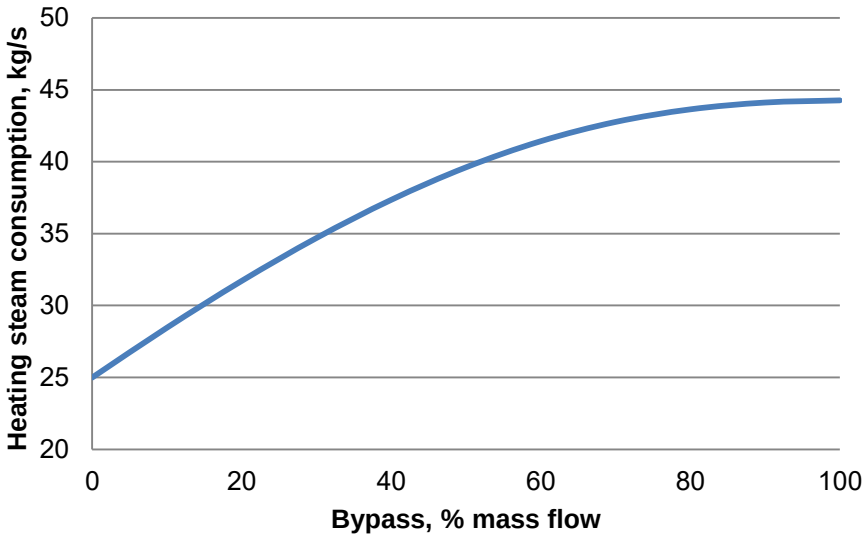

Figure 47: Heating steam consumption vs percentage bypass

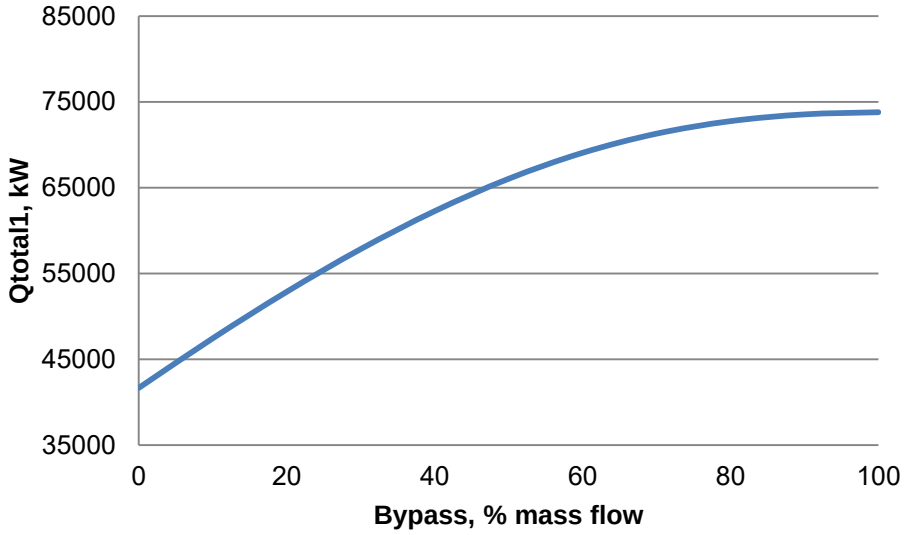

Figure 48: Total reheater heat transfer vs percentage bypass

5.2.5 MSR exit parameters with a fully bypassed moisture separator

At 100% bypass, the reheater exit parameters, without an upstream moisture separator, can be calculated and compared to exit conditions when there is no bypass of the moisture separator.

Table 6: MSR exit conditions with and without a moisture separator

	0% bypass	100% bypass
T_7, K	516,67	470,71
h_7, kJ/kg	2 923,73	2813,29
Q_{total1}, kW	41 843,94	73 785,34
TTD, K	16,48	62,44
Steam consumption, kg/s	25,11	44,27

In a scenario where the moisture separator is completely bypassed, Table 6 reflects that the reheater exit temperature and enthalpy is considerably lower with the exclusion of a separator. The steam consumption and heat transfer requirements double and the TTD declines by more than three times the design value when compared to the simulation with no bypass of the moisture separator.

6 Conclusion

This research sought to develop a mathematical model able to simulate degradation of the moisture separator component and assess this impact on the overall performance of the MSR. The model demonstrated the effects that degradation of the moisture separator has on the properties of steam exiting the moisture separator and the reheater. In addition, the effect on the MSR performance when the moisture separator is completely bypassed, was determined

Results were obtained by using the constructed model to simulate variations of degradation. The results were discussed and could be thermodynamically explained.

For both degradation conditions simulated, steam velocity was found to be the significant variable affecting all steam parameters calculated.

Although steam velocity was found to be the key variable it has limitations where, for the blockage defect, the results could not be considered past a critical upper velocity limit due to droplet behaviour at high velocities, explained by the re-entrainment theory.

Blockage of the separator channels caused elevated steam velocities through the separator and improved the moisture removal efficiency and overall MSR performance up to the critical upper velocity limit, which was calculated to correspond to a separator blockage of 14%.

As a moisture separator surface area blockage of up to 14% improves MSR performance, it can be suggested that there is margin in the separator surface area design, allowing for a reduction, which would improve the performance of the MSR and allow for a buffer against the critical re-entrainment velocity.

The model demonstrated the effect of separator blockage on moisture separator pressure differential and concluded that the improvement in moisture removal efficiency due to blocked vanes could be considered advantageous if the corresponding pressure drop is within acceptable operating limits. However, no conclusion was made as to the downstream impact to the turbine’s performance due to the lower inlet pressure.

The model demonstrated that bypass of the separator is a credible degradation condition leading to a decline in MSR performance. The steam bypass resulted in a reduction in steam velocity through the separator with a corresponding reduction in the moisture removal efficiency and a decline in the quality of steam entering the reheater.

The simulation of a fully bypassed moisture separator showed that the reheater performance declines by more than three times the design value when compared to the simulation where there is no bypass of the moisture separator.

It can be concluded that a change in MSR output could be due to separator defects where, for example, an improvement in the performance of the MSR may be due to increased blockage of separator vanes, which if not monitored and managed, could reach a critical limit where re-entrainment adversely affects MSR performance. Similarly, a decline in MSR performance may be due to moisture separator steam bypass.

In an operational scenario, a change in steam parameters at the MSR exit, with no change to inlet conditions, would lead to an investigation into the MSR internal components. Historically, fault-finding for the MSR has been focussed on the reheater and specifically the tube bundle integrity. This research demonstrates that fault-finding and possibly inspection regimes should include the moisture separator component due to the credibility of the impact separator degradation has on the MSR performance.

7 Bibliography

[1] Eskom Generation, *Nuclear Engineering Programme,* Cape Town, 2012.

[2] Y. A. Cengel, Heat Transfer A Practical Approach, Boston: McGraw-Hill, 1998.

[3] R. Amini, M. Amini, A. Jafarinia and M. Kashfi, “Numerical investigation on effects of using segmented and helical tube fins on thermal performance and efficiency of a shell and tube heat exchanger,” vol. 138, pp. 750-760, 2018.

[4] J. M. Kay and R. M. Nedderman, Fluid Mechanics and Transfer Processes, Cambridge: Cambridge University Press, 1985.

[5] S. Liu and H. Kakac, Heat exchangers. Selection, rating and thermal design, New York: CRC Press, 2002.

[6] R. W. Serth, Process Heat Transfer Principles and Applications, Elsevier, 2007.

[7] Y. A. Cengel and M. A. Boles, Thermodynamics An Engineering Approach Seventh Edition, New York: McGraw-Hill, 2011.

[8] “Nuclear-Power.net,” [Online]. Available: https://www.nuclear-power.net/nuclear-engineering/thermodynamics/laws-of-thermodynamics/thermal-efficiency/thermal-efficiency-of-rankine-cycle/. [Accessed 20 October 2019].

[9] Z. Huang, L. Qianfeng, Q. Benke, B. Hanliang and C. Feng, “Study on working mechanism of AP1000 moisture separator by numerical modeling,” *Annals of Nuclear Energy,* vol. 92, pp. 345 - 354, 2016.

[10] “Engineers Edge,” 2018. [Online]. Available: https://www.engineersedge.com/thermodynamics/typical_steam_cycle.htm. [Accessed 14 June 2018].

[11] Eskom Generation, *Moisture Separator Reheater GSS,* vol. Revision 1c, 2008.

[12] EPRI, “Moisture Separator Reheater Source Book,” 1997.

[13] Stein Industries, *Development of Designs for Moisture Separator Reheaters.*

[14] C. Yan, G. Li and J. Wang, “Optimization of a moisture separator reheater,” *Annals of Nuclear Energy,* vol. 73, pp. 537-546, 2014.

[15] J. F. Charbonnel, “Moisture Separator Reheat Systems For Nuclear Power Stations,” *Joint Power Generation Conference,* vol. 5, pp. 1-17, 1997.

[16] Filters, “http://www.filters.it,” Filters, 11 March 2016. [Online]. Available: https://www.filters.it/docs/mesh-vane-mist-eliminator/. [Accessed December 2018].

[17] J. Li, S. Huang and X. Wang, “Numerical Study of Steam-Water Separators with Wave-type Vanes,” *Chinese Journal of Chemical Engineering,* vol. 15, no. 4, pp. 492-498, 2007.

[18] M. J. Moore and C. H. Sieverding, Two-Phase Steam Flow in Turbines and Separators, Wahington: Hemisphere Publishing Corporation, 1976, pp. 318-330.

[19] S. A. Banitabaei, H. Rahimzadeh and R. Rafee, “Determinatin of minimum pressure drop at different plate spacings and air velocity in a wave-plate mist eliminator,” *Asia-Pacific Journal of Chemical Engineering,* vol. 7, pp. 590-597, 2011.

[20] “AFP Tech,” 04 February 2019. [Online]. Available: http://www.afptech.eu/vane%20packs.htm.

[21] Y. Liu and Z. Qu, “Numerical Investigation of Moisture Separators with Corrugated Plates,” *Energy Procedia,* vol. 105, pp. 1501 - 1506, 2017.

[22] “Varun Engineering,” 04 February 2019. [Online]. Available: http://www.varunengg.com/gallery.html .

[23] S. Calvert, I. L. Jashnani and S. Yung, “Entrainment Separators for Scrubbers,” *Journal of the Air Pollution Control Association,* pp. 971-975, 1974.

[24] J. P. Monat, K. J. McNulty, I. S. Michelson and O. V. Hansen, “Accurate Evaluation of Chevron Mist Eliminators,” *Chemical Engineering Progress,* p. 32–39, 1986.

[25] F. Moadron, “Modeling of a 3-zone Feedwater Heater,” ChemPlant Technology,

2013.